NASA CR-143707

Final Report

A STUDY OF UNMANNED MISSION OPPORTUNITIES TO COMETS AND ASTEROIDS

F. I. Mann
J. L. Horsewood
W. Bjorkman

Report No. 74-29
Contract NAS5-21963
December 1974

ANALYTICAL MECHANICS ASSOCIATES, INC.
10210 GREENBELT ROAD
SEABROOK, MARYLAND 20801

SUMMARY

Several unmanned multiple-target mission opportunities to comets and asteroids have been studied. The targets investigated include Grigg-Skjellerup, Giacobini-Zinner, Tuttle-Giacobini-Kresak, Borrelly, Halley, Schaumasse, Geographos, Eros, Icarus, and Toro, and the trajectories consist of purely ballistic flight, except that powered swingbys and deep space burns are employed when necessary.

Optimum solar electric rendezvous trajectories to the comets Giacobini-Zinner/85, Borrelly/87, and Tempel(2)/83 and /88 employing the 8.67 kw Sert III spacecraft modified for interplanetary flight have also been investigated.

The problem of optimizing electric propulsion heliocentric trajectories, including the effects of geocentric launch asymptote declination on launch vehicle performance capability, has been formulated and a solution has been developed using variational calculus techniques. Comparison cases have been run on the computer and the results have been presented as a paper at an AIAA conference.

Major improvements have been made to the HILTOP trajectory optimization computer program, and a report detailing the changes is being published concurrently.

An error analysis of high-thrust maneuvers involving spin-stabilized spacecraft has been developed and applied to the Synchronous Meteorological Satellite mission.

TABLE OF CONTENTS

I. INTRODUCTION

This study of unmanned multiple-target mission opportunities to comets and asteroids begins with a presentation of performance requirements for single-target comet rendezvous missions via solar electric propulsion.

Optimum solar electric rendezvous trajectories to the comets Giacobini-Zinner/85, Borrelly/87, and Tempel(2)/83 and /88 employing the 8.67 kw Sert III spacecraft modified for interplanetary flight have been investigated and the results are presented in Section II and in Appendix A. Launched by either a Titan III E/Centaur or a Shuttle/Transtage combination, the Sert III spacecraft performs rendezvous missions to one of the three comets at various points in the comet's orbit, after which the spacecraft remains with the comet indefinitely, possibly performing scientific measurements throughout the comet's period of revolution. Performance requirements and thruster throttling considerations are discussed, and an overview of the missions is presented.

Section III consists of a presentation of several multiple-target mission opportunities to comets and asteroids. Each mission investigated involves two targets and consists of an all-ballistic trajectory which returns to the vicinity of the Earth after having intercepted the initial target. At the first passage of the spacecraft by the Earth, a swingby maneuver perturbs the heliocentric trajectory either to send the spacecraft directly to the second target or to re-target the spacecraft back to the vicinity of the Earth for one or more additional swingby maneuvers. The key parameters defining the existence of these double-target-via-Earth-swingby solutions are presented in tabular form.

Section IV consists of a solution to the problem of optimizing electric propulsion heliocentric trajectories having high geocentric launch asymptote declinations. Comparison cases have been run on the computer and the results have been published [9].

Section V describes the major improvements which have been made to the HILTOP trajectory optimization computer program. A report detailing the changes is being concurrently published [10]. The program changes include the incorporation of power degradation, housekeeping power, and declination optimization into the model. The ballistic swingby-continuation simulation capability has been significantly expanded.

Section VI summarizes the transfer of the QUICKTOP III and CHEBYTOP III trajectory optimization computer programs from the NASA Ames Research Center to the Goddard Space Flight Center, and their subsequent usage.

Section VII presents the results of an error analysis of high-thrust maneuvers involving spin-stabilized spacecraft, with application to the Synchronous Meteorological Satellite mission. In addition to the simulation of the burn, an algorithm predicts the expected post-burn errors. The procedure incorporates navigational uncertainties in the pre-burn state, and attitude and magnitude errors during the burn to estimate errors in the resulting orbital elements.

II. SERT III COMET RENDEZVOUS MISSIONS

Performance requirements for rendezvous missions to three highly interesting comets which have perihelia near one astronomical unit from the sun have been investigated. Launched by either a Titan III E/Centaur or a Shuttle/Transtage combination, an 8.671 kilowatt Sert III spacecraft, modified for interplanetary flight, performs rendezvous missions to one of the three comets at various points in the comet's orbit, after which the spacecraft remains with the comet indefinitely, possibly performing scientific measurements throughout the comet's period of revolution. The comets are Giacobini-Zinner, having a perihelion passage on September 5, 1985; Borrelly, having a perihelion passage on December 18, 1987; and Tempel II, having perihelion passages on June 1, 1983 and September 16, 1988. The missions of interest are referenced to these perihelia passages.

The proposed interplanetary version of the Sert III spacecraft was simulated using the spacecraft model employed by the HILTOP trajectory optimization program [1], using parameter values suggested by the Lewis Research Center, Cleveland, Ohio [2]. In terms of the engineering parameters used by the HILTOP program, the total thrust subsystem, including power conditioners, of the Sert III spacecraft has an efficiency $\eta = .63376$, which includes the 12^{o} thrust canting angle of the three operating thrusters; this thrust subsystem accepts a (reference) power of 8.671 kilowatts, input to the power conditioners, when all three thrusters are operating at full power. The trajectory simulations of interest here do not require more than three* full-throttle thrusters operating at one time; any spare thrusters and power conditioners are therefore included in the net spacecraft mass. The Sert III spacecraft is assumed to have a constant specific impulse of 2900 seconds; in this approximation, both the efficiency and specific impulse are maintained constant with throttling ratio, whereas in reality they vary slightly with throttling ratio. The propellant tankage weight is assumed to be ten percent of the propellant weight, and these two weights vary with each

*Three is not necessarily the optimum number.

trajectory solution; reserve propellant and tankage must be accounted for in the net spacecraft mass.

The following mass components are assumed to be components of the Sert III spacecraft. Three thrusters at 16 pounds per thruster; 48 pounds: three power conditioners at 45 pounds per power conditioner; 135 pounds: solar array, 340 pounds: solar array structure and gimbals, 20 pounds: solar array orientation mechanism, 14 pounds: sun sensor on solar array, 5 pounds: computer for thruster operations, 10 pounds· and cabling, 7 pounds. These mass components add up to 579 pounds, or 262.6 kilograms, which is the "propulsion system mass" assumed by the HILTOP trajectory optimization computer program. All other mass is either propellant, tankage, or net spacecraft mass. A switching matrix between power conditioners and thrusters is omitted. Variation of the above mass component assumptions does not alter the basic results of this study; inert mass component values may be juggled between the net spacecraft mass and propulsion system mass, keeping the sum constant.

The thrust vector is assumed to be optimally oriented (along the primer vector) at each point of a given trajectory, and thrust angle limits are given in Appendix A. The optimization criterion for this study is maximum net spacecraft mass. Coast phases are optimized. Launch date, departure excess speed, and departure asymptote declination are also optimized. The effect of degradation of the solar array is ignored. Launches are from the Eastern Test Range, with an assumed latitude of $28^{\circ}.5$; the Titan III E/Centaur is assumed to have a range safety constraint corresponding to a parking orbit inclination of $32^{\circ}.5$, and the Shuttle/Transtage is assumed to have one corresponding to an inclination of 57°.

The six standard orbital elements defining the two-body motion of each comet in the ecliptic system, in astronomical units and degrees, are given by the following table:

	Giacobini-Zinner	Borrelly	Tempel II	
			1983	1988
a	3.516014	3.610604	3.035350	3.036684
e	.7075535	.6242364	.544894	.544428
i	31.87374	30.32472	12.4374	12.4317
Ω	195.20738	75.26815	119.1582	119.1183
ω	172.48223	353.33262	190.9242	191.0410
t_p	9/5.6956/85	12/18.2683/87	6/1.5342/83	9/16.7175/88

Representative trajectory profiles, projected onto the ecliptic, are displayed in Figs. 1 to 3, for missions rendezvousing at perihelion. The optimum launch dates for these trajectories are shown. Missions tend to fall into multiple-year classes, since locally optimum launch dates usually occur each year, when the Earth is in its most favorable position in its orbit, which may be approximately determined intuitively by considering the geometrical configuration of the transfer trajectory. All trajectories considered in this study are single-revolution trajectories, such as those depicted in Figs. 1 to 3, since such trajectories, to the comets considered, have minimum solar distances essentially at one astronomical unit, which considerably eases the spacecraft thermal design problem. All trajectory profiles shown are four year missions, except for one three year profile, the innermost one of Fig. 3. For trajectories which rendezvous at the same time but which depart in different years, the longer-flight-time trajectories will obviously move farther away from the sun than the shorter ones.

It can be seen that all three comets pass relatively close to the Earth's orbit when the comets are at perihelion; Giacobini-Zinner and Borrelly both recede to about six astronomical units from the sun, whereas Tempel II recedes to about 4.7 AU. In Figs. 1 and 2, the spacecraft trajectories to Giacobini-Zinner and Borrelly have maximum solar distances of about 4 AU, and in Fig. 3 the maximum solar distances are approximately in the 3 to 3½ AU

Figure 1

COMET GIACOBINI-ZINNER RENDEZVOUS MISSION
USING SERT III TECHNOLOGY

Ecliptic Projections

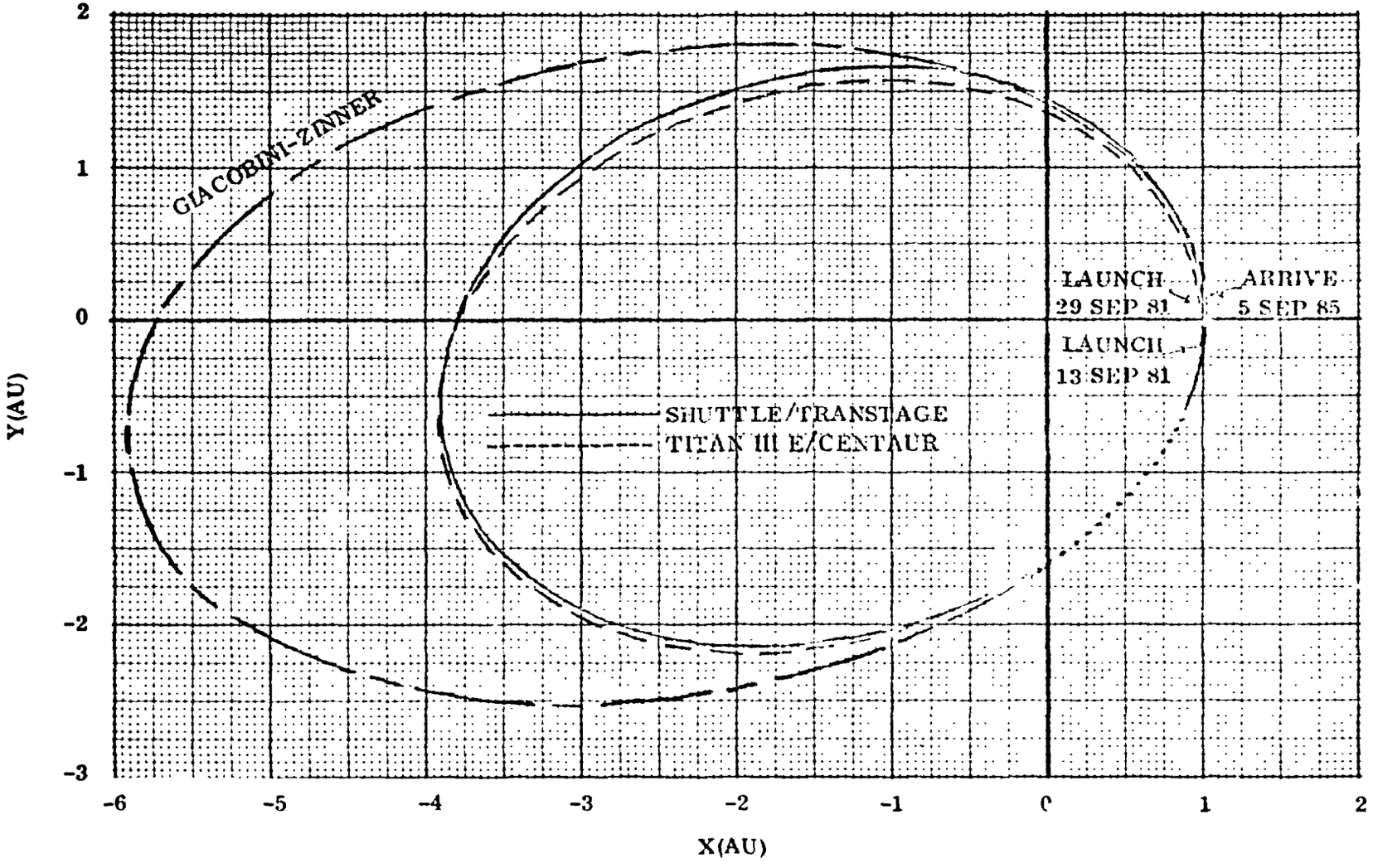

Figure 2

COMET BORRELLY RENDEZVOUS MISSION
USING SERT III TECHNOLOGY

Ecliptic Projections

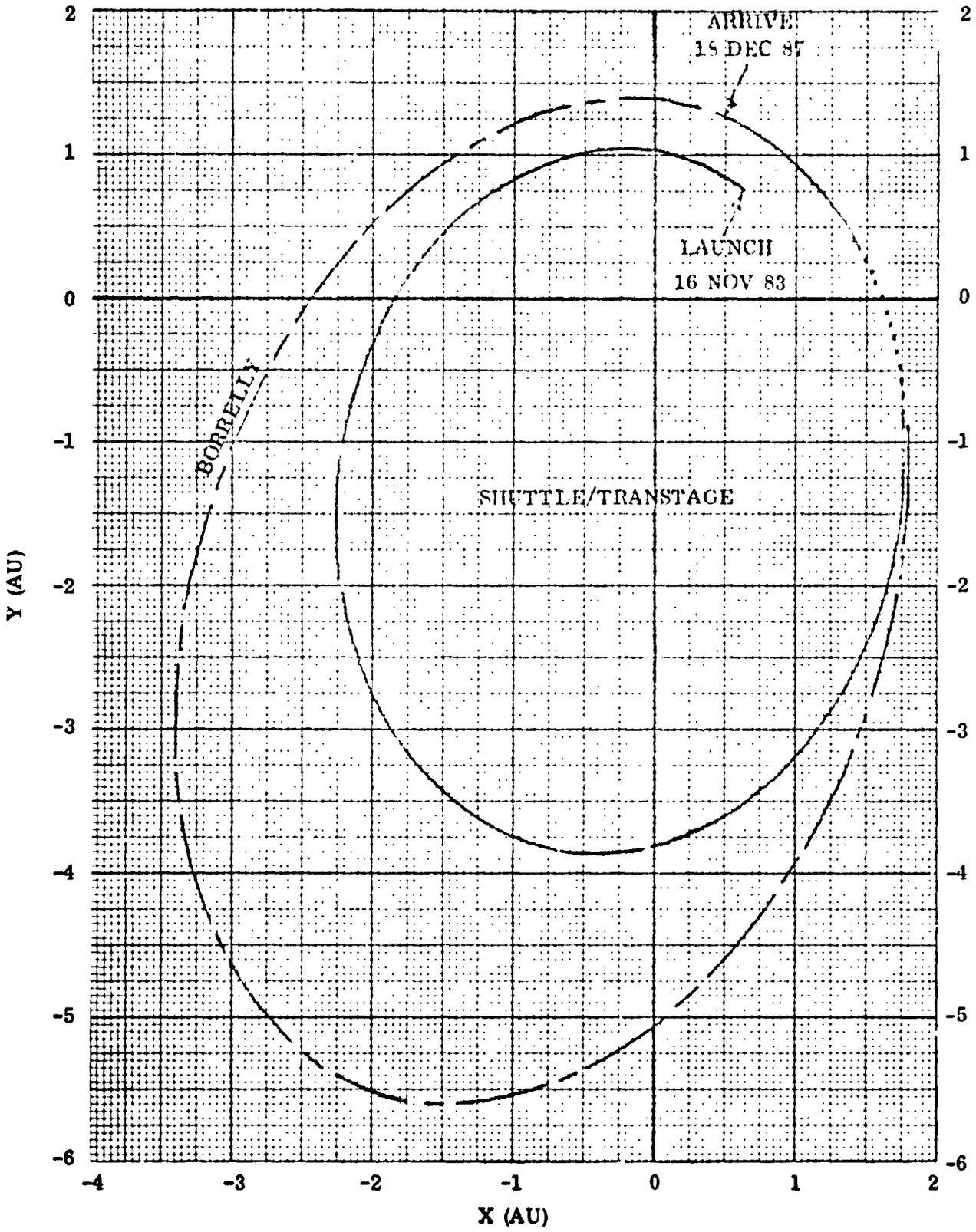

Figure 3

COMET TEMPEL II RENDEZVOUS MISSION
USING SERT III TECHNOLOGY

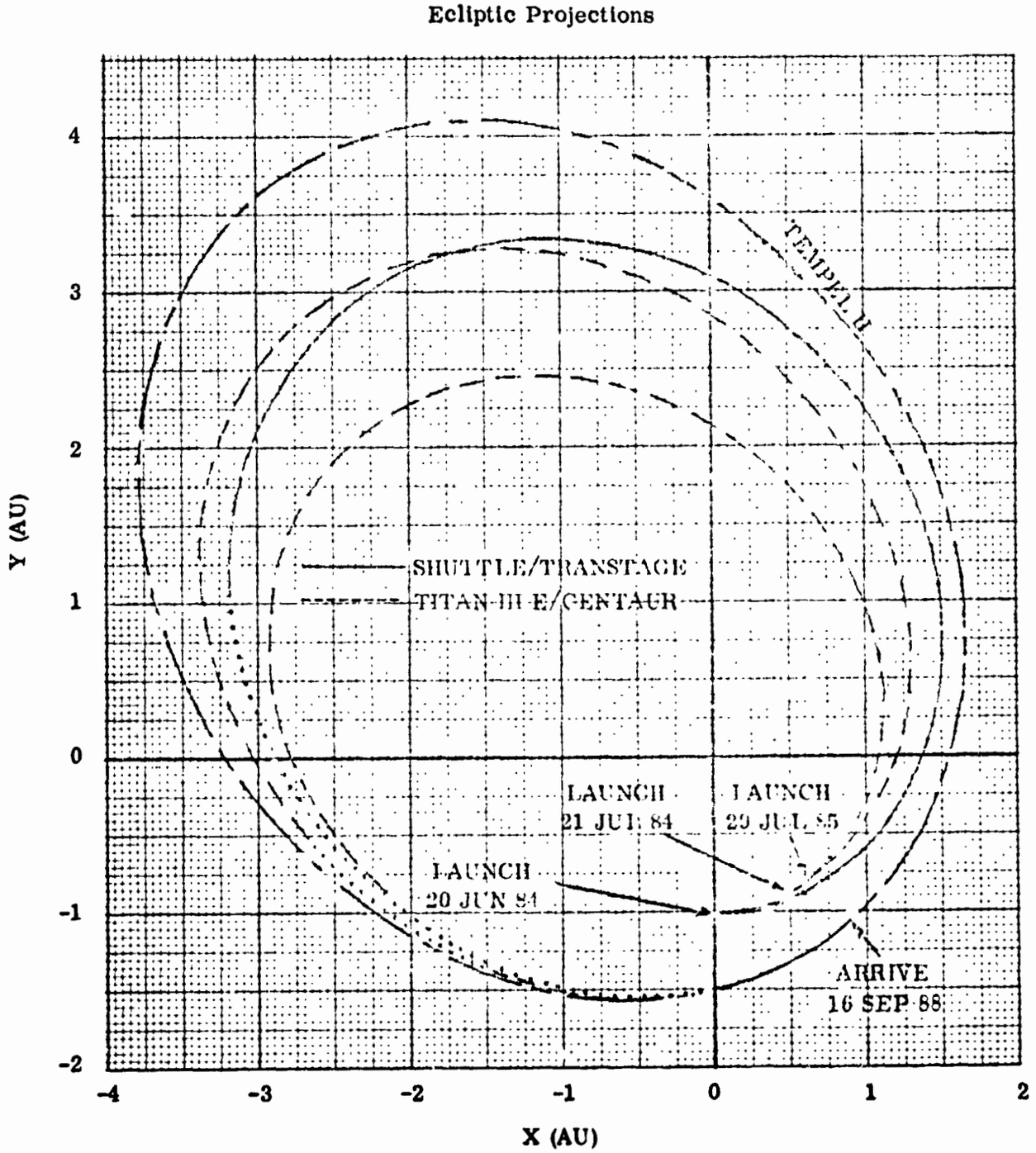

range. Detailed values of the maximum and minimum spacecraft solar distances are given in Appendix A.

Figs. 4 through 6 display the power curves, normalized to the reference power, corresponding to the trajectory profiles of Figs. 1 through 3. Gaps in the curves represent optimum coast phases. These power profiles represent the normalized solar power available to the spacecraft for propulsion along the given trajectory, since this is in accordance with the method by which the HILTOP computer program simulates trajectories. Housekeeping power is not represented, and therefore housekeeping power considerations must be included in the net spacecraft mass. The HILTOP program trajectory simulation does not employ explicit engine throttling, shutdown, and start-up along the powered portion of a trajectory, since these operations may be done implicitly, so long as the input power to the power conditioners equals the product of the reference power (8.671 kw) and the power ratio. Engine throttling considerations are therefore accomplished by utilizing normalized power curves such as those shown, and, in general, there may be more than one throttling solution available along a given trajectory. As a crude example of this, for a spacecraft having three thrusters, a power ratio of one-third at a given point along a trajectory may be satisfied, in the approximation considered here, by either one thruster at full throttle or two thrusters at one-half throttle. The particular solution having the least number of thrusters operating at any given instant is usually considered to be the best, since this solution implies a higher throttling ratio, which in turn implies slightly improved performance in the real-world model.

If the engines on board the Sert III spacecraft have a minimum throttling ratio of one-half, this corresponds to a one-half times one-third equals one-sixth, or about .167, normalized power cutoff value, below which the spacecraft must coast since there is not enough power to operate even one thruster. Considering the power profiles corresponding to the four-year missions in Figs. 4 through 6, it can be seen that this power cutoff value results in imposed

Figure 4

COMET GIACOBINI-ZINNER RENDEZVOUS MISSION
USING SERT III TECHNOLOGY

Arrival at Perihelion on 5 SEP 1985

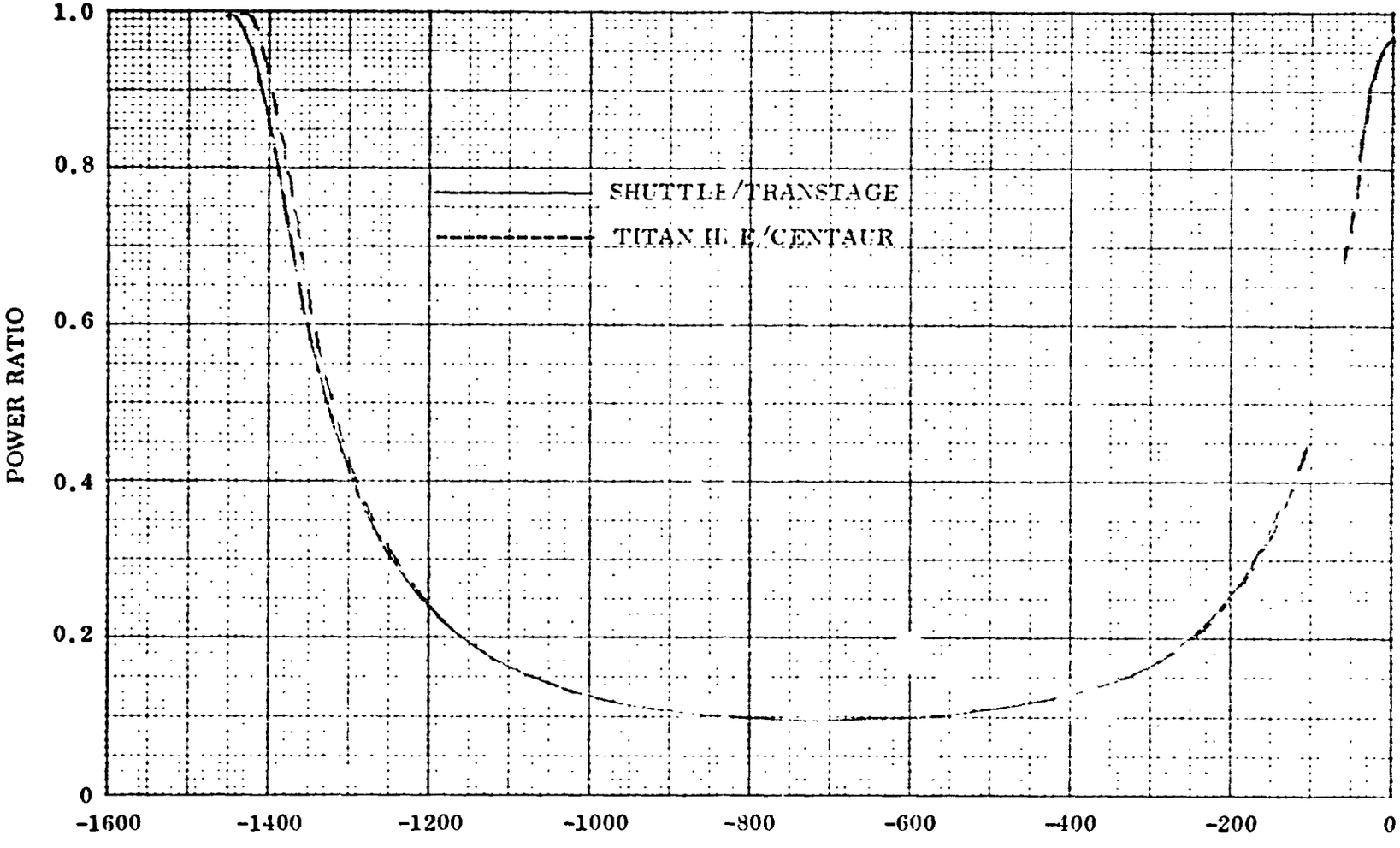

Figure 5

COMET BORRELLY RENDEZVOUS MISSION
USING SERT III TECHNOLOGY

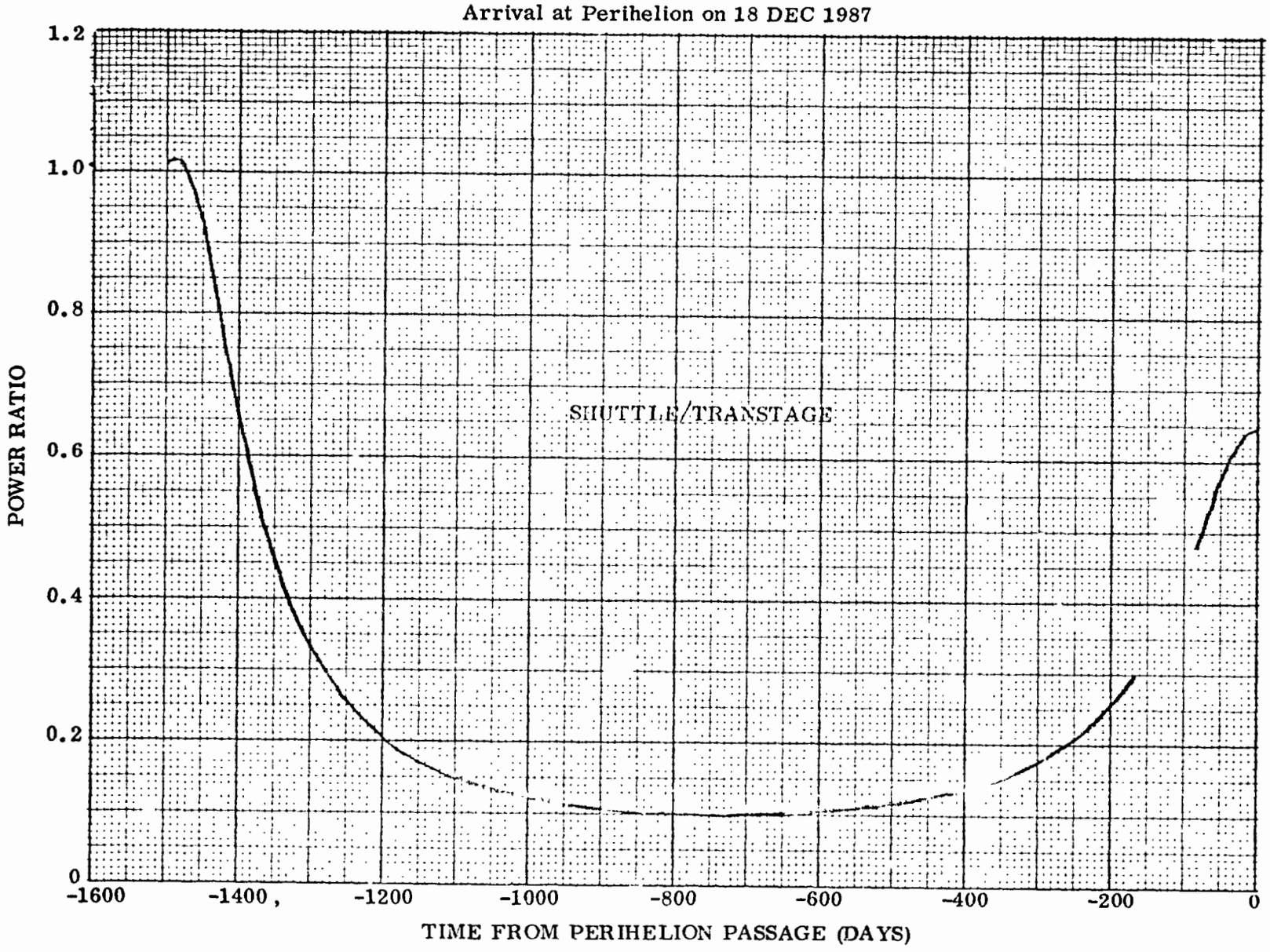

Figure 6

COMET TEMPEL II RENDEZVOUS MISSION
USING SERT III TECHNOLOGY

Arrival at Perihelion on 16 SEP 1988

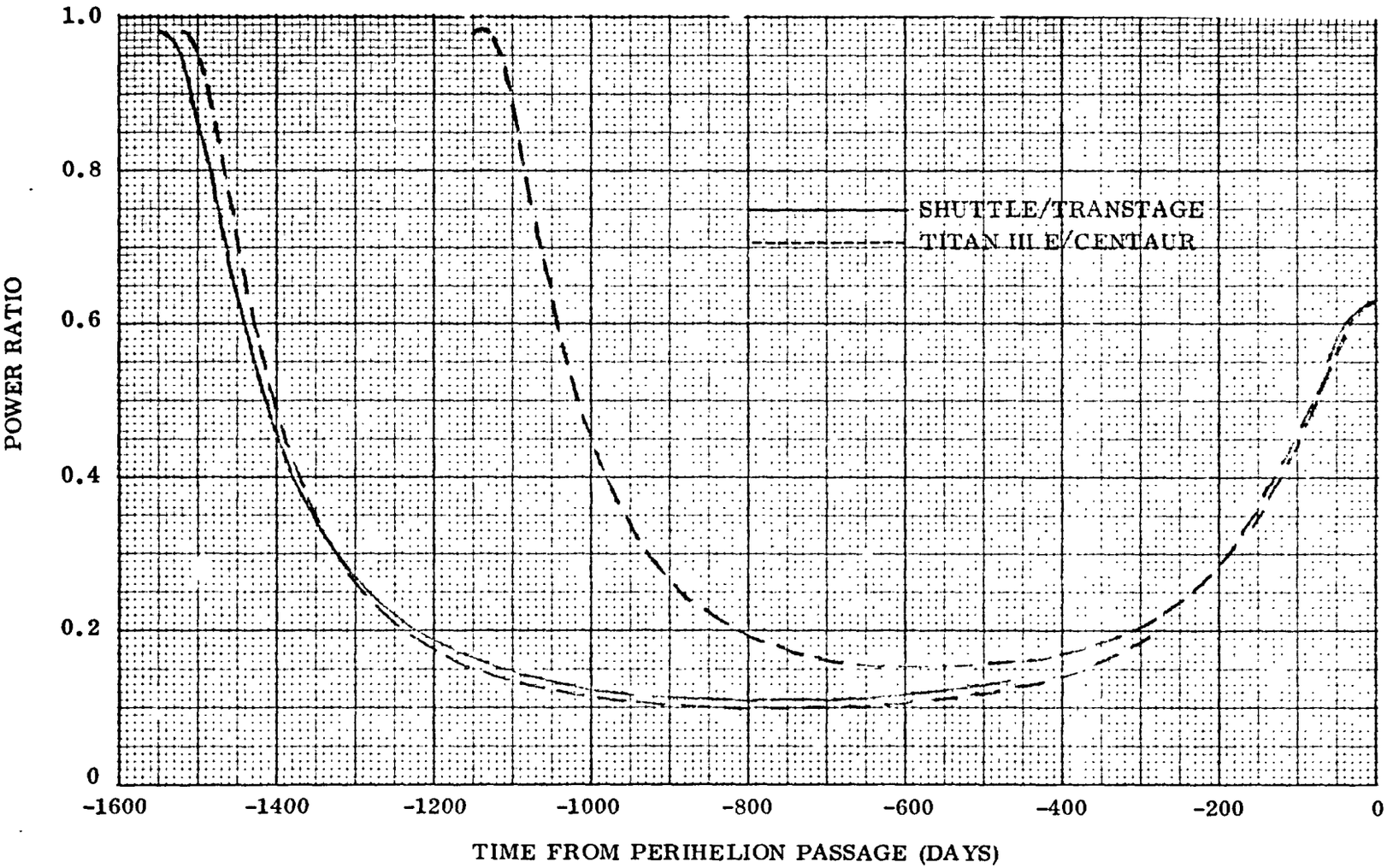

coast phases lasting for 800 to 850 days during the portion of flight which is farthest from the sun, and results in an imposed coast phase of about 300 days for the three-year mission of Fig. 6. Due to the HILTOP computer program simulation, however, the spacecraft was assumed to thrust during these times, the thrust being obviously quite weak; it is felt that this approximation does not greatly affect the results of this performance analysis study, in which the spacecraft masses, primarily the net mass, are of greatest significance. The spacecraft masses corresponding to real-world trajectories, having imposed coast phases near their aphelia, are therefore assumed to be in good approximation to those given in this report, although other mission parameters such as launch date may have to be adjusted. Also, some trajectories in this study have very brief periods after the launch time, such as in Fig. 5, during which the power ratio exceeds unity, a condition which cannot be physically satisfied by the assumed 8.671 kw Sert III spacecraft unless a fourth thruster is briefly turned on. Such optimum spacecraft trajectories could easily be adjusted, without degrading the performance significantly, so that a maximum of only three thrusters would be required.

The total propulsion system on-time for each trajectory generated is tabulated in Appendix A; however, these tabulated values merely correspond to the duration for which the spacecraft is considered to be thrusting by the HILTOP computer program, and therefore are not a realistic assessment of the actual thruster on-time, which must be determined by again considering the representative power-ratio curves as given by Figs. 4 through 6 together with the throttling lower limit of a single thruster. If this lower-limit is assumed to be one-half, then, for example, the Borrelly rendezvous power curve of Fig. 5 may be analyzed approximately as follows:

Case (1): With Imposed Coast Phase

In this case, there is an imposed coast phase from about -1140 to about -320 days from comet rendezvous, due to the lack of power available

to operate even one thruster. Since there are three thrusters, the pertinent values of power ratio are two-thirds $\cong .667$ and one-third $\cong .333$. For approximately the first 100 days, 3 thrusters must operate (after which a maximum of only two are required for the remainder of the mission), for approximately the next 100 days, 2 thrusters are on, and then one thruster operates for about 160 days up to the start of the imposed coast phase. Following the imposed coast phase, one thruster operates for about 150 days and then 2 thrusters are on for the final 80 days. This amounts to $(3 \times 100) + (2 \times 100) + (160) + (150) + (2 \times 80) = 970$ single-thruster-days, which, if shared equally by the three thrusters, implies that each thruster operates for only 323 days.

Case (2): Without Imposed Coast Phase

This case is identical to the above except for an additional 820 single-thruster-days, which increases the total single-thruster-days to 1790, which, when divided by three (thrusters), yields 597 operating days per thruster.

The Case (1) value is considered to be more representative, but may have to be adjusted upward slightly when the imposed coast phase is actually introduced into the simulation. The Borrelly-rendezvous power-curve discussed as an example is representative of most power profiles for four-year missions involved in this comet rendezvous study, and, since thruster on-time values are generally less for three year and two year missions, the general conclusion may be drawn that the maximum thruster on-time for each thruster of the Sert III spacecraft will be "about one year", a situation which will of course improve if a fourth "spare" thruster is available to equally share the load.

Were a fourth thruster to have been assumed in the HILTOP trajectory simulation, then the reference power assumed by HILTOP would have been 4/3 as great as that actually assumed. Consequently, the optimization algorithm, sensing a more powerful electric propulsion spacecraft, would have directed the launch vehicle to inject more initial mass (and, for low power levels, more net mass) into heliocentric space at less departure excess speed, requiring the

electric propulsion spacecraft to bear more of the burden in effecting the rendezvous, and involving some adjustment to the trajectory profile. This process of adding more thrusters, or discrete steps of reference power, increases the net mass up to a point, which would be as close as the discrete reference-power variation could get to the true optimum value of reference power, which varies with launch vehicle.

Some of the comet rendezvous mission simulations employed a new theory for the optimization of the launch asymptote declination, which is discussed in Section IV. Most of the Borrelly missions, some of the Giacobini-Zinner missions, but none of the Tempel II missions made use of the new launch optimization model. The results of the launch phase optimization are summarized by the tabulations of the launch asymptote declination δ and the parking orbit inclination i in Appendix A.

A performance overview for the Sert III comet rendezvous missions is displayed in Fig. 7, in which the top of each bar represents the net spacecraft mass deliverable to perihelion rendezvous, each notch below the top corresponds to the net mass rendezvous capability at 50, 100, 150, ... etc. days before perihelion, and each bar above the top shows the net mass rendezvous capability at 50, 100, 150, ... etc. days after perihelion.

The most striking feature of this bar graph is the relatively large net masses which the little Sert III spacecraft is capable of rendezvousing with Tempel II during the 1988 opportunity. As solar system targets go, these three comets are relatively easy to get to, since they pass somewhat near to the Earth's orbit. However, as may be seen by examining the comet's orbital elements listed earlier in this section, Tempel II is inclined only about 12^{o} to the ecliptic, whereas Giacobini-Zinner and Borrelly are in the 30^{o} range. Moreover, the value of Tempel II's semi-major axis, which is proportional to its energy, is closer to the Earth's value than those of the other two comets. These facts are considered to be the major contributing factors in the explanation of the greater Tempel II/1988 net mass capability.

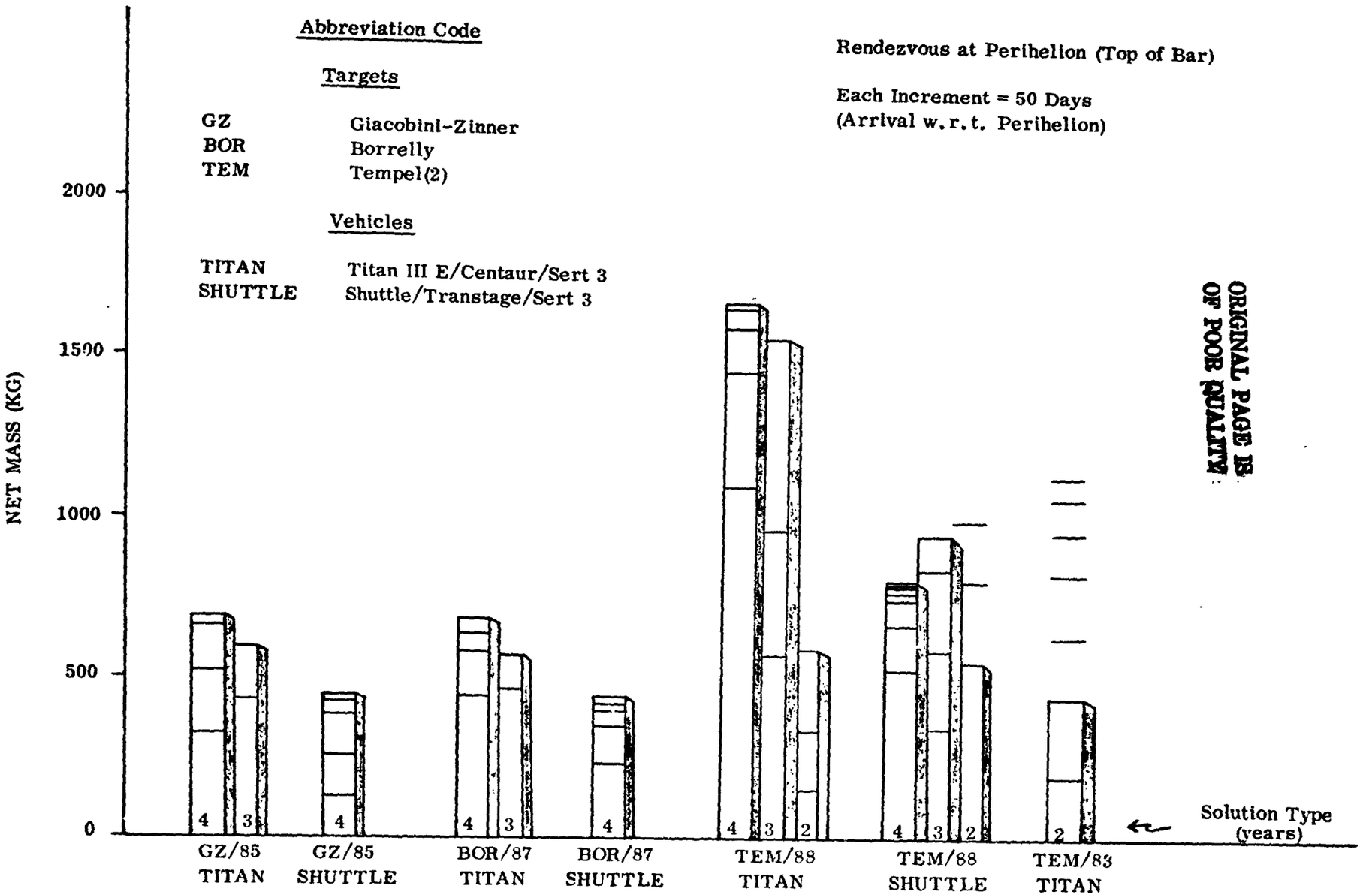

Figure 7. Performance Overview for Missions to the Three Selected Targets.

Considering the TEM/88 TITAN bars of Fig. 7, there is only a small penalty in net mass between the 4-year mission and the 3-year mission, rendezvousing at perihelion; however, when considering rendezvousing fifty, or one hundred, days before perihelion, the penalty is seen to be severe for the 3-year mission, but small for the 4-year mission, and this is basically because the 3-year mission is more difficult for the little Sert III spacecraft to accomplish. Clearly there is a trade-off between mission duration and payload delivered, to produce a minimum-cost mission for accomplishing given scientific objectives.

Another obvious fact derivable from Fig. 7 is the lesser interplanetary capability of the Shuttle/Transtage relative to the Titan III E/Centaur; what is not obvious is the relative launch costs, which hopefully would be less for the Shuttle.

Only the 2-year Tempel II/1983 mission was investigated, due to the unlikelyhood of a comet rendezvous electric propulsion mission being launched before 1981; hence the emphasis on post-perihelion rendezvous, which not only yield greater net masses delivered but also are associated with later launch dates.

Detailed tabular data pertaining to these comet rendezvous missions may be found in Appendix A.

III. BALLISTIC MULTIPLE-TARGET FLYBY MISSIONS*

The work described in this section consisted of confirming the existence of ballistic multiple-target mission opportunities to comets and asteroids, in particular those which pass relatively near to the Earth's orbit, such that one or more Earth-swingby maneuvers can be employed to perturb the heliocentric trajectory. Details of the Earth swingby technique and complete descriptions of the multiple-target mission profiles are discussed by Farquhar, et. al. [11, 12].

All missions involve two targets and consist of trajectories which return to the vicinity of the Earth after having intercepted the first target. At the first passage of the Earth, a swingby maneuver perturbs the heliocentric trajectory either to send the spacecraft directly to the second target or to re-target the spacecraft back to the vicinity of the Earth for one or more additional swingbys, in which the final swingby sends the spacecraft to the second target. Quite often there is more than one way to swing past the Earth at a given Earth-passage, in order to produce the desired re-targeting of the spacecraft.

This work was accomplished using the HILTOP trajectory optimization computer program [1, 10]. This program generates swingby maneuvers under the assumption of the patched-conic approximation, such that the swingby planet's sphere-of-influence is assumed to have zero radius as seen from interplanetary space and infinite radius as seen from the planetary vantage point. The passage time in the swingby planet's sphere-of-influence is neglected, i.e., taken to be zero in the heliocentric reference frame.

When, for a particular multiple-target mission, no trajectory solution could be found having entirely unpowered swingby maneuvers, powered swingby maneuvers were employed, and the minimum ΔV solution was determined in each case by optimizing the post-swingby-leg flight time. Figure 8 depicts the relation of unpowered swingby solutions to the wider class of powered swingby

*The multiple-target missions described in this section were originally identified by R.W. Farquhar of the Goddard Space Flight Center.

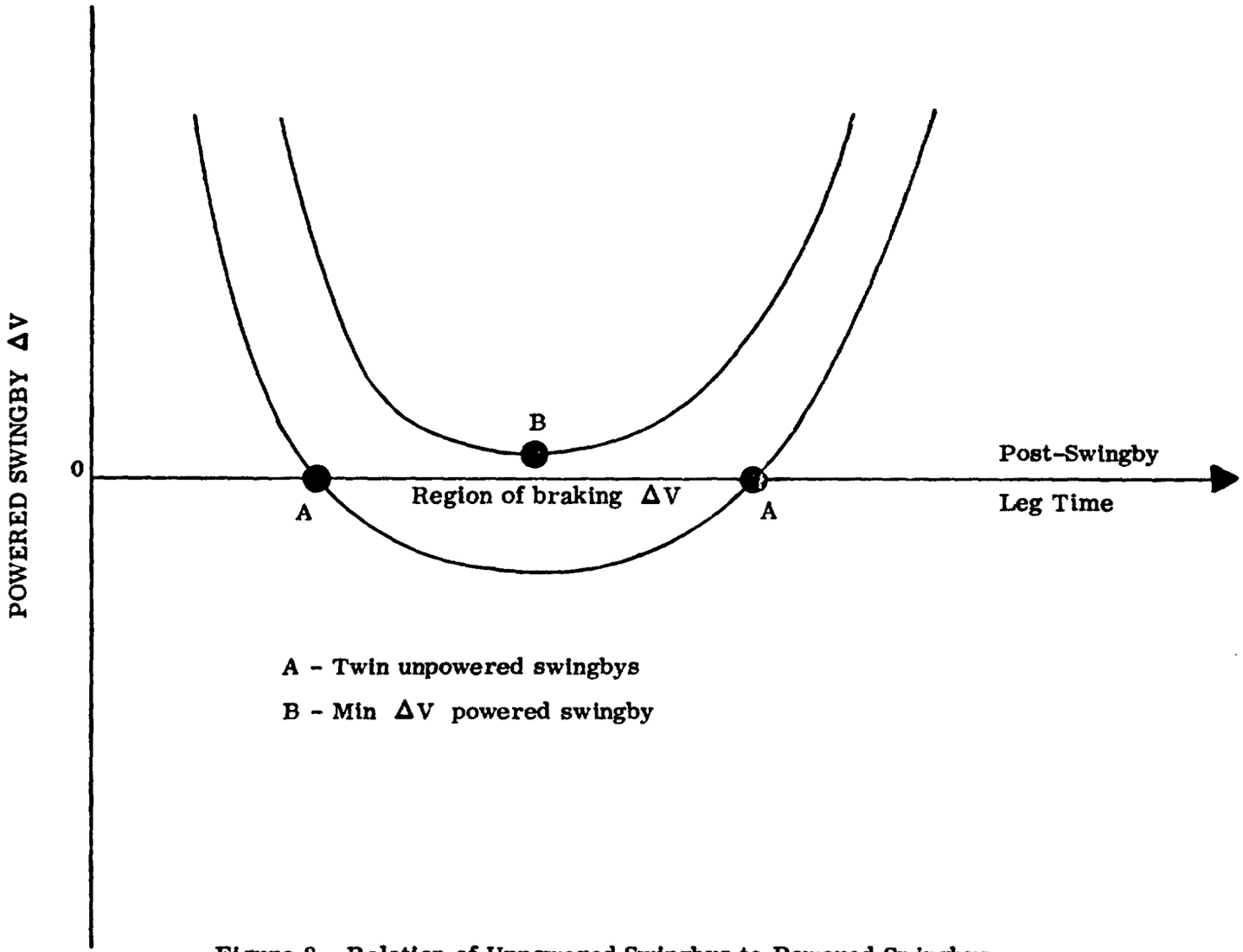

Figure 8. Relation of Unpowered Swingbys to Powered Swingbys.

solutions. The upper curve represents the case in which no unpowered swingbys exist, and the lower curve shows how unpowered swingbys occur in pairs, even though one or both of the corresponding trajectories may hit the swingby planet.

Each powered swingby maneuver is constrained to occur at the mutual perifoci of the approach and departure hyperbolic trajectory segments within the swingby planet's sphere of influence; the burn is assumed to be impulsive with the thrust collinear to the velocity at closest approach.

The first-target (of a double-target sequence) investigated in this study was either the 1977 apparition of the comet Grigg-Skjellerup (GS/77), the 1982 apparition of the same (GS/82), or the 1985 apparition of the comet Giacobini-Zinner (GZ/85). The spacecraft thus launches from the Earth, flies past one of these comets at considerable relative speed, and returns to the vicinity of the Earth to perform a swingby maneuver onto a subsequent target. For convenience, the following abbreviations are used for three of the comets:

GS	Grigg-Skjellerup
GZ	Giacobini-Zinner
TGK	Tuttle-Giacobini-Kresak

An overview of the double-target missions investigated is given in Table III-1, and the six standard orbital elements defining the two-body motion of the targets involved, in the ecliptic system, expressed in astronomical units and degrees, are given in Table III-2.

Table III-3 contains the parameters which characterize the initial heliocentric trajectory segments including launch from Earth, flyby of the initial target, and arrival back at Earth, for the three cases investigated (GS/77, GS/82, GZ/85). In each case, the initial target is approximately crossing the ecliptic at the time of encounter, and the trajectory segments are essentially 360° in-ecliptic transfers. The trajectory segments defined by Table III-3 apply to all of the associated missions to second-targets, summarized by Table III-1 (except for the unpowered swingby to Halley, in which the spacecraft returns to swingby the Earth after three

TABLE III - 1

OVERVIEW OF MISSIONS INVESTIGATED

First Target	Second Target	No. of Earth Swingbys	Comments
GS/77	GZ/79	1	Min ΔV powered swingby.
	ICARUS/78	1	Two unpowered swingby possibilities.
GS/82	TGK/84	1	Two unpowered swingby possibilities.
	GEOGRAPHOS/83	1	Three unpowered swingby possibilities, one having relatively low flyby speed at Geographos (9.3 km/sec).
	TORO/83	1	Possibility of unpowered or min ΔV powered swingby.
	ICARUS/87	1	Min ΔV powered swingby.
	SCHAUMASSE/84	1	Min ΔV Earth powered swingby followed by Min ΔV Venus powered swingby.
	HALLEY	1	Min ΔV powered swingby (or lone unpowered swingby using a three year transfer to Earth).
GZ/85	BORRELLY/87	2	First swingby is standoff encounter; second Earth encounter has two unpowered swingby possibilities.
	TORO/87	1	Powered swingby having Earth passage distance 1.2 radii.
	EROS/87	1	Family of powered swingbys having low flyby speeds at Eros (4 to 6 km/sec).
	ICARUS/87	1	Lone unpowered swingby.
	GEOGRAPHOS/87	1	Lone unpowered swingby.

TABLE III - 2

TARGET ORBITAL ELEMENTS

Target	a	e	i	Ω	ω	t_p
BORRELLY/87	3.61060400	.6242364	30.32472	75.26815	353.33262	12/18.26830/87
EROS/87	1.45820548	.2227330	10.82860	304.30050	178.55830	5/23.75410/87
GEOGRAPHOS/83	1.24472390	.3420300	13.33410	337.23520	276.54530	5/18.77180/83
GEOGRAPHOS/87	1.24495016	.3420090	13.32880	337.26210	276.54740	7/18.76370/87
GS/77	2.96273200	.6647010	21.10145	213.03235	359.31610	4/11.00088/77
GS/82	2.95889800	.6656651	21.13392	213.09221	359.32122	5/14.99629/82
GZ/79	3.49071500	.7146548	31.69660	195.47830	171.96939	2/12.91951/79
GZ/85	3.51601400	.7075535	31.87374	195.20738	172.48223	9/ 5.69583/85
HALLEY	17.94348000	.9672770	162.24046	58.67151	111.87092	2/ 9.39474/86
ICARUS/78	1.07785100	.8267308	22.92507	87.95981	31.10711	5/28.72346/78
ICARUS/87	1.07795840	.8266640	22.88890	88.00800	31.18870	5/11.87700/87
SCHAUMASSE/84	4.08725300	.7032880	11.84050	80.42600	57.38400	12/ 7.36721/84
TGK/84	3.14693400	.6430245	9.93305	153.73014	49.52093	7/28.41270/84
TORO/83	1.36737860	.4511330	9.37360	274.27700	126.81560	12/16.39710/83
TORO/87	1.36736120	.4511070	9.37290	274.30820	126.80780	2/26.47011/87

Orbital elements obtained from Dr. D.K. Yeomans of Computer Sciences Corporation.

TABLE III - 3

PARAMETERS CHARACTERIZING INITIAL TRAJECTORY SEGMENTS

EARTH LAUNCH	INITIAL TARGET FLYBY	EARTH ARRIVAL
	GS/77	
Date = 10/30/76 C_3 = 2.3 km^2/sec^2 δ = $-18^o.5$	Date = 4/11/77 Flyby at 15.2 km/sec CD = .20 AU CA = 82^o	Date = 10/30/77 V_∞ = 1.53 km/sec
	GS/82	
Date = 10/23/81 C_3 = 8.0 km^2/sec^2 δ = $9^o.9$	Date = 5/15/82 Flyby at 15.3 km/sec CD = .37 AU CA = 76^o	Date = 10/24/82 V_∞ = 2.83 km/sec
	GZ/85	
Date = 3/10/85 C_3 = 12.3 km^2/sec^2 δ = $-4^o.1$	Date = 9/11/85 Flyby at 20.6 km/sec CD = .46 AU CA = 80^o	Date = 3/10/86 V_∞ = 3.51 km/sec

NOMENCLATURE

δ - Departure asymptote declination
CD - Communication distance
CA - Communication angle (Sun = 0^o)

years instead of one, with the trajectory to GS being the same). Therefore, it would be theoretically possible to send several spacecraft, perhaps using a single launch, to, say, GS/82 to obtain several different viewpoints of the comet, and each spacecraft could subsequently swing past the Earth differently and continue on to a different target.

Parameters defining the trajectory segments which continue from Earth swingby to the final targets are given in Tables III-4, III-5, and III-6. These tables, together with Table III-3, completely define the double-target missions which have been identified. It is helpful to refer back to the comments in Table III-1 in order to better understand the latter tables. Multiple swingby possibilities (at the same time) are specified by multiple-values, for certain parameters, which are separated by slashes.

The GZ/85: Eros/87 double-target mission consists of a family of possibilities having relatively slow flybys of Eros. This family of missions, in which the post-swingby-leg transfer time is varied, is summarized by Figure 9.

TABLE III - 4

PARAMETERS CHARACTERIZING FINAL TRAJECTORY SEGMENTS

FOR GS/77 MISSIONS

EARTH SWINGBY	SECOND-TARGET FLYBY
	GZ/79
R = 3.21 ΔV = 392 meters/sec	Date = 2/19/79 Flyby at 20.9 km/sec CD = 1.83 AU CA = 23°
	ICARUS/78
R = ..96/31.27 ΔV = zero/zero meters/sec	Dates = (7/15/78)/(7/24/78) Flyby at 29.5/26.3 km/sec CD = .51/.65 AU CA = 82°/87°

NOMENCLATURE

R	Passage distance (Earth radii)
ΔV	Powered swingby incremental velocity
CD	Communication distance
CA	Communication angle (Sun = 0°)

(Also applies to Tables III - 5 and III - 6)

TABLE III - 5

PARAMETERS CHARACTERIZING FINAL TRAJECTORY SEGMENTS

FOR GS/82 MISSIONS

EARTH SWINGBY	SECOND-TARGET FLYBY
R = 14.97/1.46 ΔV = zero/zero meters/sec	TGK/84 Dates = (6/12/84)/(6/21/84) Flyby at 14.5/15.6 km/sec CD = 1.80/1.77 AU CA = 43°/42°
R = 3.07/3.76/12.34 ΔV = zero/zero/zero meters/sec	GEOGRAPHOS/83 Dates = (3/16/83)/(7/2/83)/(11/29/84) Flyby at 13.9/9.3/12.5 km/sec CD = .10/.62/1.53 AU CA = 120°/66°/39°
R = 1.38/6.47 ΔV = 63/zero meters/sec	TORO/83 Dates = (9/29/83)/(2/13/84) Flyby at 10.1/12.8 km/sec CD = 1.19/.35 AU CA = 65°/90°
R = 1.81 ΔV = 1014 meters/sec	ICARUS/87 Date = 4/1/84 Flyby at 25.0 km/sec CD = 1.79 AU CA = 60°

TABLE III - 5 (continued)

EARTH SWINGBY	SECOND-TARGET FLYBY
Earth Swingby to Venus R = 8.86 ΔV = 404 meters/sec Venus Swingby Date = 2/10/84 R = 1.42 Venus radii ΔV = 950 meters/sec	SCHAUMASSE/84 Date = 10/17/84 Flyby at 12.2 km/sec CD = 1.37 AU CA = 69°
R = 17.27/7.10 ΔV = 120/zero meters/sec	HALLEY Dates = (3/15/85)/(3/8/85) Flyby at 71.8/78.2 km/sec

TABLE III - 6

PARAMETERS CHARACTERIZING FINAL TRAJECTORY SEGMENTS

FOR GZ/85 MISSIONS

EARTH SWINGBY	SECOND-TARGET FLYBY
First Passage R = 64.05 ΔV = zero meters/sec Second Passage Date = 8/20/87 R = 3.54/3.45 ΔV = zero/zero meters/sec	BORRELLY/87 Dates = (12/25/87)/(12/30/87) Flyby at 17.3/17.3 km/sec CD = .53/.56 AU CA = 125^{o}/122^{o}
R = 1.20 ΔV = 17 meters/sec	TORO/87 Date = 4/20/87 Flyby at 15.7 km/sec CD = 1.42 AU CA = 44^{o}
R = 5.39 ΔV = 220 meters/sec (Min) (see Figure 9)	EROS/87 Date = 5/6/87 Flyby at 6.3 km/sec CD = 1.84 AU CA = 33^{o}
R = 13.78 ΔV = zero meters/sec	ICARUS/87 Date = 6/19/87 Flyby at 30.7 km/sec CD = .16 AU CA = 59^{o}
R = 3.79 ΔV = zero meters/sec	GEOGRAPHOS/87 Date = 9/26/87 Flyby at 12.9 km/sec CD = .40 AU CA = 90^{o}

Figure 9

FAMILY OF EROS SLOW FLYBYS

IV. LAUNCH ASYMPTOTE DECLINATION OPTIMIZATION

Introduction. Preliminary performance studies of heliocentric electric propulsion missions require some means of correlating initial spacecraft mass m_o and launch hyperbolic excess velocity V_∞. In most studies to date, this has been accomplished by equating m_o to the launch vehicle (LV) payload m_ℓ, which is represented as a non-linear function of the scalar quantity v_∞, the hyperbolic excess speed. With few exceptions, this LV payload capability assumed has been that corresponding to a due-East launch from the ETR. The direction of the launch hyperbolic excess velocity is usually left unspecified and is determined as part of the solution to the optimization problem. Using the indirect optimization technique, the solution dictates that V_∞ be directed along the initial primer vector, a requirement that may be in conflict with the assumed LV payload capability.

By properly choosing the point of the (coplanar) injection from a circular parking orbit, the geocentric declination δ of the hyperbolic excess velocity may lie within the range

$$-i \leq \delta \leq i, \qquad (1)^*$$

where i is the equatorial inclination of the parking orbit established by the launch vehicle. If the launch excess velocity asymptote declination, as determined by the solution to the optimization problem, falls within this range and if the LV payload capability is compatible with the orbit inclination i, then the solution is consistent within the assumptions made and the results are valid. However, if $|\delta| > i$, then the basic assumptions regarding LV capability are in conflict, and it is necessary to formulate the optimization problem to account for the dependence of LV payload on direction of the launch excess velocity asymptote.

Although the questionable validity of published high asymptote declination solutions has been recognized for some time, no formal treatment of the problem

*Equation numbers referenced in this section of the report pertain to this section only.

has been noted in the literature. The authors had previously developed[1] a technique for adjusting the LV payload to account for the non-coplanar injection maneuver required to achieve the geocentric declination of the primer vector, which was colinear with V_∞, but this a posteriori correction approach has proven unacceptable because the original transversality conditions (TC's) were no longer valid. Typically, these TC's resulted in "solutions" which were not stationary points. This condition arose because the alignment of V_∞ with the initial primer was no longer a necessary condition of optimality, but rather an imposed constraint which was in violation of the assumptions used in originally formulating the solution.

In this discussion, a unified treatment of the high asymptote declination problem is presented. The LV payload capability is modeled as a function not only of the magnitude of V_∞ but also of the inclination of the circular parking orbit and of the declination of the launch asymptote. The formulation permits the optimization of both the parking orbit inclination and asymptote declination or of the asymptote declination subject to a limitation on parking orbit inclination to satisfy range safety constraints. The necessary conditions of optimality are derived for a typical comet or asteroid rendezvous problem.

Problem Formulation. High asymptote declinations frequently arise in missions to targets that have orbits highly inclined to the ecliptic, such as those to certain comets and asteroids. Therefore, we select, for illustrative purposes, an optimal rendezvous mission to a single, massless target whose path is defined by a specified ephemeris. The extension of the results derived here to other missions of interest, such as flybys, orbiters, and multiple-target missions, is straightforward. We shall also assume a propulsion system of fixed size in terms of mass and reference power Also, overall propulsion system efficiency and the specific impulse of the thruster subsystem are assumed given and are held constant throughout the mission.

The assumed spacecraft and propulsion system models are as described in [1] and will not be repeated here. The launch vehicle payload capability is assumed to follow the simple exponential law

$$m_\ell = b_1 e^{-(v_c/b_2)} - b_3, \tag{2}$$

where b_1, b_2, and b_3 are pre-determined constants for each launch vehicle and v_c is a characteristic speed representative of the energy required to achieve a specific escape trajectory. For example, for a due-East launch from ETR and a coplanar injection maneuver, v_c is defined to be the speed required at departure from a low altitude circular reference orbit to achieve a specified hyperbolic excess speed v_∞, i.e.,

$$v_c = \sqrt{v_\infty^2 + 2v_o^2}\ , \tag{3}$$

where v_o is the circular satellite speed in the reference orbit. Thus, for due-East launches and coplanar injection maneuvers, m_ℓ is a function only of v_∞ for a given launch vehicle. Performance data for a large selection of existing and potential launch vehicles are presented graphically in Reference [3] as a function of v_c, as defined above, with the reference orbit altitude being 185 kilometers. The authors have found a least-squares curve fit to the exponential law above using, say, 7-10 data points from a given payload curve to be a quite adequate and accurate representation of a launch vehicle's performance capability.

To accomodate large launch asymptote declinations, the same exponential law for launch vehicle payload may be used, but the definition of characteristic speed must be expanded to reflect the additional energy required to rotate the asymptote. This new definition of v_c is taken to be that given above plus the velocity penalties associated with the asymptote rotation. The rotation is assumed to be accomplished by first choosing a launch azimuth which establishes a given reference orbit inclination i followed by a non-coplanar injection

maneuver from that circular reference orbit to the desired asymptote, as illustrated in the figure on the following page. The velocity penalty incurred with non-due-East launches from the ETR is shown graphically in Reference [3] as a function of the orbit inclination. This velocity penalty, which we will denote Δv_i is adequately approximated with a quadratic curve fit of the form

$$\Delta v_i = c_1 i^2 + c_2 i + c_3. \tag{4}$$

Normal range safety limitations restrict the range of inclinations achievable through varying the launch azimuth alone. The referenced graph indicates that the maximum allowable northerly azimuth will yield an orbital inclination of about 48.5 degrees while the maximum allowable southerly azimuth will yield an inclination of about 32 degrees. Now, given a reference orbit inclination i, it remains to define the velocity penalty Δv_g associated with a non-coplanar departure from this circular orbit to the desired hyperbolic excess velocity at a declination δ. Assuming the line of nodes of this reference orbit is an open variable, one may choose this variable to minimize the angle between the excess velocity and the orbital plane. This minimum angle is $\delta - i$. Gunther[4] has shown that the minimum incremental velocity required to achieve a given v_∞ along an asymptote not lying in the orbital plane from a specified circular orbit is obtained from the solution to a quartic equation in the sine of the out-of-plane angle. Defining

$$s = \sin(\delta - i); \quad \rho = v_\infty / v_o;$$

$$p = s^2 (\rho^2 + 4);$$

$$q = s^2 (1 - s^2) \rho^2; \tag{5}$$

$$x = \left[\sqrt{(q/2)^2 + (p/3)^3} + q/2\right]^{\frac{1}{3}} - \left[\sqrt{(q/2)^2 + (p/3)^3} - q/2\right]^{\frac{1}{3}};$$

LAUNCH GEOMETRY

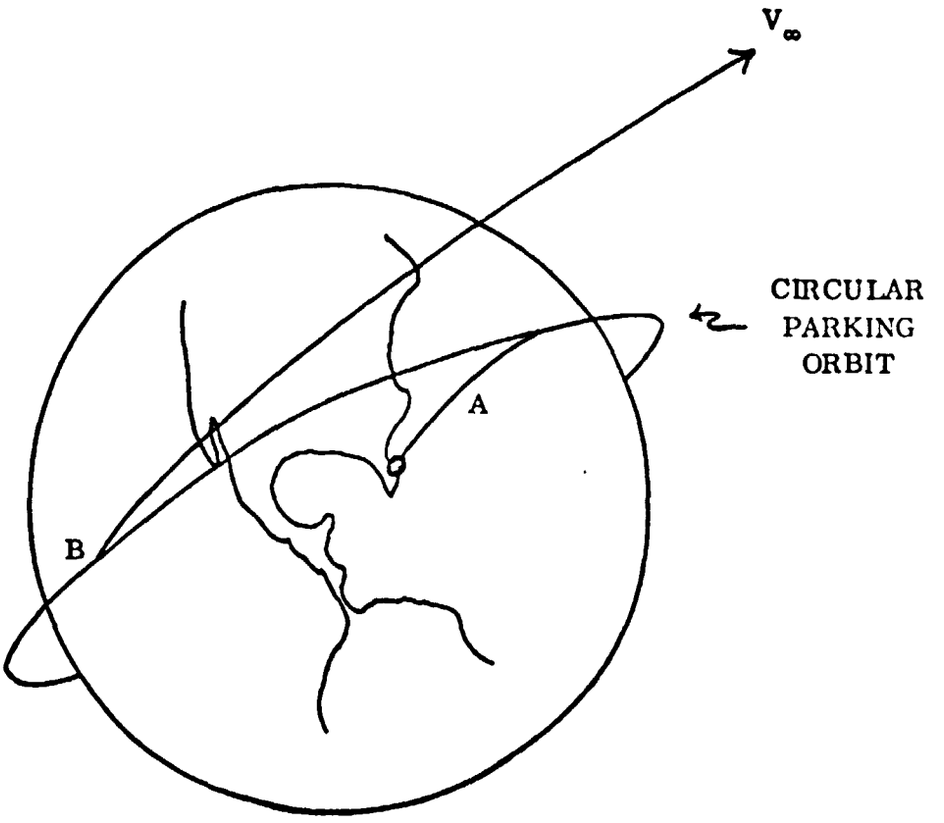

(A) NON DUE EAST LAUNCH INTO PARKING ORBIT

(B) OPTIMUM NON COPLANAR BURN OUT OF PARKING ORBIT

$$y = \sqrt{\rho^2/4 - x}\ ;$$

$$w = \frac{1}{2}\left[\rho/2 + y + \sqrt{(\rho/2+y)^2 + 4\left(x/2 + \sqrt{x^2/4 + s^2}\right)}\ \right], \qquad (5)\ \text{cont.}$$

then Gunther's solution for the magnitude of the minimum velocity impulse required to accomplish the maneuver is

$$v_g = v_o \sqrt{\rho^2 + 3 - 2\sqrt{(1 + \rho w - w^2)(2 + \rho w)}}\ , \qquad (6)$$

and the penalty Δv_g is the difference between v_g and the velocity increment required if the out-of-plane angle were zero, i.e.,

$$\Delta v_g = v_g - \left(\sqrt{v_\infty^2 + 2v_o^2} - v_o\right).$$

Thus, the definition of the characteristic speed for those cases in which the asymptote declination lies outside the interval (1) is

$$v_c = \sqrt{v_\infty^2 + 2v_o^2} + \Delta v_i + \Delta v_g$$

$$= v_o + v_g + \Delta v_i\ . \qquad (7)$$

Optimality Conditions. The state and adjoint equations for the problem under consideration are precisely as formulated in Ref. [1]. The only difference in the optimality conditions is the format and content of certain of the transversality conditions. Specifically, these differences are due solely to the new definition of v_c which is now a function of the direction of V_∞ as well as its magnitude. Whereas before the differential of v_c was, simply

$$dv_c = (v_\infty/v_c)\, dv_\infty\ ,$$

we see from (7) that the equivalent formula now is

$$dv_c = (\partial v_g/\partial v_\infty)\, dv_\infty + (\partial v_g/\partial \delta)\, d\delta$$

$$+ (\partial v_g/\partial i + \partial \Delta v_i/\partial i)\, di$$

where, from (4)

$$\partial \Delta v_l / \partial i = 2 c_1 i + c_2 ,$$

and, from (5) and (6)

$$\partial v_g / \partial i = - \partial v_g / \partial \delta .$$

The derivation of the partial derivatives $\partial v_g / \partial v_\infty$ and $\partial v_g / \partial \delta$ is straightforward although somewhat cumbersome. The equations are presented in Appendix B.

After noting that the differential of g, the reference thrust acceleration, is

$$dg = - (g/m_l)\, dm_l$$

where

$$dm_l = - (b_1/b_2)\, e^{-(v_c/b_2)}\, dv_c ,$$

and that the differential of V_∞ may be written

$$dV_\infty = (V_\infty/v_\infty) dv_\infty + (\bar{n}_p \times V_\infty) d\alpha + [(V_\infty \times \bar{n}_p) \times V_\infty / |V_\infty \times \bar{n}_p|\,]\, d\delta ,$$

where $\bar{n}_p$ is a unit vector along the North Pole and α is the geocentric right ascension of V_∞, one may write the transversality conditions associated with V_∞ by inspection.

For optimum launch parking orbit inclination:

$$f(\partial \Delta v_l / \partial i - \partial v_g / \partial \delta) = 0 . \qquad (8)$$

For optimum launch excess speed:

$$f(\partial v_g / \partial v_\infty) - (\Lambda_o \cdot V_\infty)/v_\infty = 0 . \qquad (9)$$

For optimum launch asymptote declination:

$$f(\partial v_g / \partial \delta) - \Lambda_o \cdot [(V_\infty \times \bar{n}_p) \times V_\infty / |V_\infty \times \bar{n}_p|\,] = 0. \qquad (10)$$

For optimum launch asymptote right ascension:

$$-\Lambda_o \cdot (\bar{n}_p \times V_\infty) = 0 . \tag{11}$$

In the above equations Λ_o is the initial primer vector and f is

$$f = [k_s + k_t - (1 + k_t)\nu_f - g\lambda_g / m_\ell] \, dm_\ell / dv_c ,$$

where k_s and k_t are the structural and tankage factors, respectively, ν_f is the final mass ratio, and λ_g is the final value of the Lagrange multiplier associated with reference thrust acceleration.

Equation (11) implies that the right ascension of V_∞ must be equal to, or 180 degrees from, that of Λ_o; i.e., V_∞ must lie in the plane of Λ_o and $\bar{n}_p$. If the first term in (10) were zero, which is the result obtained when the effects of declination are ignored in the formulation, then one obtains from (10) and (11) the familiar result that V_∞ must be colinear with Λ_o. Usually it is assumed that V_∞ is aligned with Λ_o, however, cases have been found [5] for which the optimum solution resulted in V_∞ being diametrically opposed to Λ_o. The fact that the first term in (10) is non-zero means that V_∞ will be offset from Λ_o by a finite angle. This offset, as noted above, must be in the plane of Λ_o and $\bar{n}_p$ and, intuitively, we know it must be in the direction of the equator so as to reduce v_c. The amount of the offset of V_∞ from Λ_o may not be determined from (11) as an initial value problem since the variable f is a function of variables (ν and λ_g) evaluated at the final time. Thus, δ must be treated as an additional independent parameter, and (10) becomes another condition to be satisfied in the boundary value problem.

The satisfaction of (8) requires that the term within parentheses vanishes since f will normally be a non-zero quantity. Therefore, since the two partial derivatives are functions only of initial conditions, one may solve for the i that causes the parenthesized term to vanish and thereby eliminate the condition (8)

from the boundary value problem. Due to the complexity of the equations defining $\partial v_g/\partial \delta$, this solution for i must be obtained using an iterative technique.

The approach to the solution of the problem as formulated above differs in three basic respects from that of the problem where asymptote declination is ignored: (1) the condition (8) must be solved for the optimum parking orbit inclination, given values of v_∞ and δ; (2) the asymptote declination δ must be introduced as an independent parameter and (10) added as an end condition of the problem; and (3) the evaluation of V_∞ becomes somewhat more involved. The computation of V_∞ given v_∞, Λ_o and δ, proceeds as follows. Denote as ϵ the obliquity of the ecliptic such that the matrix

$$\Phi = \begin{bmatrix} 1 & 0 & 0 \\ 0 & \cos\epsilon & -\sin\epsilon \\ 0 & \sin\epsilon & \cos\epsilon \end{bmatrix},$$

operating on a vector expressed in ecliptic Cartesian coordinates yields the same vector in Earth equatorial coordinates. Then the right ascension α_λ of the initial primer Λ_o may be written

$$\alpha_\lambda = \tan^{-1}\left[(\lambda_{yo}\cos\epsilon - \lambda_{zo}\sin\epsilon)/\lambda_{xo}\right],$$

where λ_{xo}, λ_{yo}, λ_{zo} are the given ecliptic coordinates of Λ_o. Then, the right ascension of the asymptote is set

$$\alpha = \alpha_\lambda \quad \text{or} \quad \alpha = \alpha_\lambda + \pi,$$

and V_∞ is evaluated

$$V_\infty = v_\infty \Phi^T \begin{bmatrix} \cos\alpha\cos\delta \\ \sin\alpha\cos\delta \\ \sin\delta \end{bmatrix}$$

This may be contrasted with the usual definition of V_∞:

$$V_\infty = v_\infty \Lambda_o / |\Lambda_o|.$$

V. HILTOP COMPUTER PROGRAM IMPROVEMENTS

This section describes the modifications and improvements made to the HILTOP electric propulsion trajectory optimization computer program [1]. New program features include the simulation of power degradation, housekeeping power, launch asymptote declination optimization, and powered and unpowered ballistic multiple swingby missions with an optional deep space burn.

Power Degradation. The power degradation model has been hypothesized by the authors in earlier publications [5, 8]. The model allows a single parameter (denoted "characteristic degradation time") to describe the power degradation behavior of an electric propulsion spacecraft to a degree which fundamentally affects the solution to the trajectory optimization problem. In short, the power generated is degraded by a multiplicative damage factor q of the form

$$q = e^{-s/\tau_d},$$

where τ_d is the characteristic degradation time and s is the degradation time, which is computed in the HILTOP program as the time integral of the density of damaging particles impinging on the solar arrays (for solar electric propulsion). The density of damaging particles is assumed to be a function of solar distance and array orientation.

The characteristic degradation time τ_d is an engineering parameter that is determined experimentally. For example, by exposing a solar cell to the particle emission of a solar simulator and measuring the performance of the cell over a period of time, a reasonable value of τ_d can be estimated.

The assumed exponential form of the degradation factor, although intended for use with SEP systems, is applicable for NEP systems as well. The principal difference is in the definition of $\dot{s}$. The exponential form permits the evaluation of radio-isotope systems by defining $\dot{s} = 1$ and letting

τ_d represent the time for the radioactivity to dissipate to 1/e of its initial level. A more complete exposition of this subject is given in [8].

Housekeeping Power . An option of simulating spacecraft housekeeping power has been added to the program. This option applies to solar electric propulsion with specified reference power. The housekeeping power is a specified constant power generated by the solar arrays and shunted away from the thruster power-conditioners and directly to the spacecraft payload for "housekeeping" purposes. The spacecraft model has been expanded by deleting the old, total propulsion system specific mass and replacing it with the specific mass of the solar arrays and the specific mass of the thruster subsystem.

Declination Optimization . The program has been expanded to include the optimization of launch asymptote declination. The launch asymptote declination optimization model was first hypothesized by the authors in the appendix of [1], and later a more thorough treatment of the subject was put forth in [9]. A solution to the problem of optimizing electric propulsion heliocentric trajectories, including the effects of geocentric launch asymptote declination on launch vehicle performance capability, has been developed using variational calculus techniques. The model of the launch vehicle performance includes a penalty associated with a non-easterly launch plus another penalty arising from a non-coplanar launch from the parking orbit. Provisions for range safety constraints are included. Optimal trajectories will generally have the launch excess velocity offset from the initial primer vector. The analysis describing the launch asymptote declination optimization model is found in Section IV of this document.

Swingby Continuation . Additional optional computations have been provided in which ballistic swingbys past the primary target may be simulated.

In one mode of program operation, single swingbys past the primary target may be simulated to up to ten post-swingby targets per case. This mode of operation was already in existence.

In another mode of program operation, multiple swingbys along a single trajectory may be simulated, first swinging past the primary target and then subsequently swinging past more targets downstream along the trajectory. One multiple swingby trajectory may be simulated per case. This mode of operation was recently added to the program.

In either mode of operation, the following basic assumptions are made. The swingby continuation computations are independent of the trajectory leg leading up to the swingby target, which may consist of an optimized electric propulsion trajectory segment (if the swingby target is the primary target), except that the arrival V_∞ and arrival time at the swingby target are used in the determination of the swingby passage conditions. Each swingby maneuver is calculated under the assumption of the patched-conic approximation, and the swingby planet's sphere-of-influence is assumed to have zero radius as seen from interplanetary space and infinite radius as seen from the planetary vantage point. The passage time in the swingby planet's sphere-of-influence is neglected (taken to be zero in the heliocentric frame).

Each swingby maneuver may be either unpowered or powered. The unpowered swingby solutions are embedded in the wider class of powered-swingby solutions, tending to appear in pairs which are separated by a region of braking powered swingbys.

The powered swingby maneuver is restricted to occur at the mutual perifoci of the approach and departure hyperbolic arcs; the powered phase is impulsive and the thrust is collinear (pro or con) to the velocity at closest approach. Whether the swingby is powered or unpowered, the trajectory segment leading up to the swingby planet has been pre-determined, this being the method by which the program has been designed to obtain swingby solutions. Therefore the swingby time and the arrival hyperbolic excess velocity are known.

A basic assumption of the powered swingby algorithm used by the program is that the flight time from the swingby planet to the next target is

specified. This being so, the program is able to converge, by iteration, on some ballistic trajectory from the swingby planet to the next target having the specified transfer time, implying that the departure hyperbolic excess velocity at the swingby planet is thereby determined. Therefore, the heliocentric trajectory before and after the swingby planet is determined, and it then remains to perform the required computations pertaining to the hyperbolic arcs within the swingby planet's sphere of influence. The computations are outlined in a companion document [10] which is being published concurrently with this report.

The unpowered swingby maneuver is considered to be a powered swingby having $\Delta V = 0$. The program adjusts the post-swingby heliocentric trajectory segment, by iteration, until the swingby departure V_∞ magnitude equals the given arrival V_∞ magnitude. The primary independent variable in this iteration is the post-swingby transfer time to the specified target, which was held constant in the powered swingby case.

The program can generate multiple-revolution ballistic arcs, and a particular solution obtained by the program may not be unique, even for the same transfer time. All solutions are reachable, however, by means of inputting an appropriate initial velocity guess for the trajectory segment in question.

Deep Space Burn. In simulations of trajectories which are all-ballistic, the program is now capable of simulating a single deep space burn, or impulsive velocity-change, at any point prior to arrival at the primary target. The three components of the incremental velocity ΔV are independent variables of the boundary value problem, such that, at a specified time, the spacecraft velocity is incremented:

$$\dot{R}^+ = \dot{R}^- + \Delta V$$

The optional existence of a deep space burn provides greater targeting flexibility in simulations of multiple target missions.

V_∞ Optimization in LVI Mode. The optimization of the launch excess velocity V_∞ when using the Launch Vehicle Independent (LVI) mode of simulation is accomplished when the initial primer vector is forced to vanish:

$$\Lambda_o = 0.$$

This is accomplished by setting the values of these three independent variables of the boundary value problem to zero and turning their triggers off; the three components of the departure heliocentric velocity become independent variables instead. The program has been augmented with special logic to circumvent the numerical singularity associated with the null primer vector.

Print Expansion. The standard trajectory block print has been expanded to include target-relative position and velocity coordinates of the spacecraft, and comet nuclear and total magnitudes as seen by both the spacecraft and Earth. A more detailed description is given in [10].

Extra-Ecliptic Missions. Extra-ecliptic mission simulations now involve launches from the Earth in which the Earth's ephemeris is generated by the program's analytic ephemeris capability; previously, extra-ecliptic missions were generated simply by starting the trajectory on the x-axis at one astronomical unit from the sun. This improved extra-ecliptic capability allows the launch date to be optimized together with the launch asymptote declination. Also, an additional set of boundary conditions has been added to the program for simulating extra-ecliptic missions, and these are given in [10].

Miscellaneous Improvements. Ephemerides for several additional comets and asteroids have been included in the program's analytic ephemeris capability, increasing the total number of possible targets to fifty-one. The ephemeris arrays have been expanded to allow up to seventy targets.

The program option of generating a ballistic trajectory as an initial guess for an electric propulsion mission has been expanded to allow multiple-revolution trajectories.

The capability has been added of monitoring the proximity of any given spacecraft trajectory to any object in the solar system.

Another capability has been added of specifying enforced coast phases for selected intervals throughout a given mission.

Finally, a major size-reduction of the HILTOP program was completed, from 436K to 326K hexadecimal locations, a reduction of 25%, allowing faster turn-around time on the GSFC IBM 360/91.

VI. QUICKTOP III/CHEBYTOP III COMPUTER PROGRAM USAGE

The QUICKTOP III[6] and CHEBYTOP III[7] computer programs have been obtained from the NASA Ames Research Center, Moffett Field, California, and converted to run on the IBM 360/91 computer at the Goddard Space Flight Center. These trajectory optimization computer programs were used initially in the Sert III comet rendezvous mission study discussed in Section II, and aided in establishing the feasibility of using the Sert III spacecraft for these comet rendezvous missions. However, it was determined early in the study that the QUICKTOP/CHEBYTOP programs were consuming as much or more machine time as the HILTOP[1] program. For this reason, a decision was made to solely use the HILTOP program for the comet rendezvous study, since the authors are more familiar with this computer program. The QUICKTOP/CHEBYTOP computer programs remain ready for use at the Goddard Space Flight Center by any interested persons.

VII. ERROR ANALYSIS OF HIGH-THRUST MANEUVERS

High thrust burns can result in large postburn errors when applied to spin-stabilized spacecraft. In addition to the simulation of the burn, an algorithm predicts the expected errors after high thrust maneuvers. The procedure incorporates navigational uncertainties in the pre-burn state, and attitude and magnitude errors during the burn to estimate errors in the resulting orbital elements. The work was performed by W. Bjorkman.

To add to the concreteness of the analytical development, the Synchronous Meteorological Satellite (SMS) mission is discussed as a sample case. The apogee burn of the SMS mission is performed by firing the solid rocket of a spin-stabilized spacecraft near apogee of the transfer orbit. The rocket burns for about 23 seconds, imparting a delta-velocity of about 1723 m/sec along the direction of the spin axis. The time of firing the rocket and the attitude of the spin axis are controllable. Appropriate values for these control parameters (firing time and attitude angles) can be determined from a scanning procedure. Any procedure used to establish control parameters will use "best estimates" of the transfer orbit state and the expected delta-velocity from the rocket. The estimated transfer orbit state will always differ from the true orbit state because of navigation errors (i.e., errors caused by neglected error sources, incomplete modeling or measurement errors in the orbit determination process). The solid rocket will not deliver exactly the delta-velocity stated by the manufacturer. In addition to these errors, the knowledge of spin-axis attitude will be in error by uncertainties in the attitude determination process. An algorithm was developed for assessing the effects of navigation errors and burn errors (i.e., delta-velocity and attitude determination errors) on the achievement of mission objectives. Attitude control errors are not considered, nor are errors in firing time. The algorithm makes use of an impulsive burn model and linear propagation of errors through the burn. A particular set of mission objectives is assumed without assuming a linear relationship between mission constraint parameter variations and navigation/burn errors. The validity of the linear error propagation assumption is

demonstrated with a numerical example.

Navigation errors are specified by means of a 6x6 covariance matrix, P_o, referred to th anchor epoch, t_o, and a suitable coordinate frame. P_o should include uncertainties due to all orbit determination errors, and not simply those uncertainties caused by measurement noise. The Cartesian state error, $\tilde{x}_o$, is the difference between the true state at epoch and the "anchor vector". We assume

$$\mathcal{E}(\tilde{x}_o) = 0 \tag{1}$$

and

$$\mathcal{E}(\tilde{x}_o \tilde{x}_o^T) = P_o \tag{2}$$

where $\mathcal{E}$ is the expectation operator. References to equations in this section of the report apply to equations in this section only. Small deviations in the state propagate linearly along the transfer orbit between t_o and the firing time, t_f, by means of the "mean conic" state transition matrix, $\varphi(t_f; t_o)$.

$$\tilde{x}_f = \varphi(t_f; t_o)\, \tilde{x}_o \tag{3}$$

This transition matrix is evaluated from the anchor vector and the osculating state (integrated from the anchor vector) at t_f, using the average reciprocal semi-major axis at the two terminals in calculation of the incremental regularizing anomaly. Table VII -1 illustrates numerically the adequacy of equation (3) for propagation of errors along the SMS-A transfer orbit. Linearity errors may be smaller than those shown in the table, because a coordinate system inconsistency was detected after the tabulated data were generated. The transition matrix is deterministic and therefore commutes with the expectation operator.

$$\mathcal{E}(\varphi \tilde{x}_o) = \varphi \mathcal{E}(\tilde{x}_o) = 0 \tag{4}$$

$$P_f = \mathcal{E}(\tilde{x}_f \tilde{x}_f^T) = \varphi \mathcal{E}(\tilde{x}_o \tilde{x}_o^T) \varphi^T = \varphi P_o \varphi^T \tag{5}$$

The effect of navigation errors on the state at firing time is thus given by P_f in equation (5).

Table VII-1

Linear Propagation Verification: Navigation Errors

$XA = \varphi \tilde{x}_o$ ($\tilde{x}_o$ = sampled anchor state error)

$$XE = XA - \left(\int_{t_o}^{t_f} f(X_o + \tilde{x}_o)\, d\tau - \int_{t_o}^{t_f} f(X_o)\, d\tau \right)$$

(In km and km/sec)

Sample		$\underline{x}$	$\underline{y}$	$\underline{z}$	$\underline{\dot{x}}$	$\underline{\dot{y}}$	$\underline{\dot{z}}$
1	XA	-45.075	23.360	-10.467	-.004850	-.001307	-.000422
	XE	- .222	- .200	- .126	.000006	-.000030	-.000001
4	XA	-107.654	52.460	-26.032	-.011686	-.003109	-.001038
	XE	- .481	- .402	- .307	.000016	-.000056	-.000004
6	XA	-119.620	48.834	-26.970	-.012252	-.004161	-.000833
	XE	- .493	- .440	- .323	.000023	-.000055	-.000002
7	XA	-43.151	21.762	-10.155	-.004660	-.001251	-.000408
	XE	- .208	- .194	- .118	.000006	-.000028	-.000001

Apogee burn errors are specified as "proportional" and "pointing" errors. The proportional error is a delta-velocity error which is proportional to the expected total delta-velocity, $\overline{\Delta V}$. Random behavior is assigned to the proportional error.

$$\mathcal{E}(k_v) = 0 \tag{6}$$

$$\mathcal{E}(k_v^2) = \sigma_v^2 \, |\overline{\Delta V}|^2 \tag{7}$$

Attitude errors contribute a delta-velocity error approximately in the plane normal to $\overline{\Delta V}$. Unit basis vectors in that plane are defined by

$$\hat{E} = \frac{1}{\sqrt{\overline{\delta v}_1^{\,2} + \overline{\delta v}_2^{\,2}}} \begin{pmatrix} -\overline{\delta v}_2 \\ \overline{\delta v}_1 \\ 0 \end{pmatrix} \tag{8}$$

and

$$\hat{N} = \frac{\overline{\Delta V}}{|\overline{\Delta V}|} \times \hat{E} \tag{9}$$

Pointing error is a circular error probability number assigned to attitude determination accuracy. It is treated as having a normal distribution about zero mean in each of two orthogonal directions.

$$\mathcal{E}(k_e) = \mathcal{E}(k_n) = 0 \tag{10}$$

$$\mathcal{E}(k_e^2) = \mathcal{E}(k_n^2) = \sigma_a^2 \, |\overline{\Delta V}|^2 \tag{11}$$

The delta-velocity vector (with errors included) may be written

$$\Delta V = (|\overline{\Delta V}| + k_v) \left[\frac{\overline{\Delta V} + k_e \hat{E} + k_n \hat{N}}{|\overline{\Delta V} + k_e \hat{E} + k_n \hat{N}|} \right] \tag{12}$$

To linearize the burn we write the delta-velocity error in the form

$$\tilde{\Delta V} = M \begin{pmatrix} r_v \\ r_e \\ r_n \end{pmatrix} = M \tilde{r} \tag{13}$$

where r_v, r_e and r_n are uncorrelated random numbers of zero mean and unit variance, defining

$$\begin{pmatrix} k_v \\ k_e \\ k_n \end{pmatrix} = |\overline{\Delta V}| \begin{pmatrix} \sigma_v r_v \\ \sigma_a r_e \\ \sigma_a r_n \end{pmatrix} \tag{14}$$

The covariance matrix of delta-velocity errors is

$$\mathcal{E}(\tilde{\Delta V}\ \tilde{\Delta V}^T) = M \mathcal{E}(\tilde{r}\tilde{r}^T) M^T = M M^T \tag{15}$$

where M is defined by the following equation

$$M = \frac{\partial \Delta V}{\partial (r_v, r_e, r_n)} \Bigg|_{r_v = r_e = r_n = 0}$$

$$= |\overline{\Delta V}| \left(\sigma_v \frac{\overline{\Delta V}}{|\overline{\Delta V}|} \quad \sigma_a \hat{E} \quad \sigma_a \hat{N} \right) \tag{16}$$

The adequacy of the linear model for burn errors is illustrated numerically in Table VII -2. The comparisons were obtained by multiplying random samples of $\tilde{r}$ by M of equation (16) and differencing these with (ΔV of equation (12) - $\overline{\Delta V}$). The input standard deviations were: $\sigma_v = .0025$ and $\sigma_a = (.43/57.3)^o$.

Table VII -2

Linear Propagation Verification: Burn Errors

$$XA = M\,\tilde{r}$$
$$XE = XA - (\Delta V - \overline{\Delta V})$$

(In meters/second)

Sample		ε_x	ε_y	ε_z
1	XA	.3336	-.0109	-.3015
	XE	-.0000	-.0001	.0000
2	XA	-.8110	1.5135	.7079
	XE	-.0001	- .0001	-.0000
3	XA	2.6601	-7.2964	-3.6459
	XE	.0022	.0004	.0010

The post-burn state is computed impulsively by adding ΔV to the pre-burn velocity.

$$X^+ = X_f + \begin{pmatrix} 0 \\ \Delta V \end{pmatrix} \tag{17}$$

Errors are added the same way,

$$\tilde{x}^+ = \tilde{x}_f + \begin{pmatrix} 0 \\ \tilde{\Delta V} \end{pmatrix} \tag{18}$$

The covariance matrix of post-burn errors, P^+, is then computed adding $\varepsilon(\tilde{\Delta V}\ \tilde{\Delta V}^T)$ of equation (15) to P_f of equation (5). Navigation and burn errors are assumed uncorrelated.

$$P^+ = P_f + \begin{bmatrix} 0 & 0 \\ 0 & MM^T \end{bmatrix} \tag{19}$$

A vector, ψ, of mission constraint parameters was defined for the SMS mission. Each element of ψ can be computed unambiguously from X^+. The parameters are:

ψ_1 required three-impulse trim velocity required to circularize at synchronous radius with a specified inclination and node

ψ_2 longitudinal drift rate

ψ_3 eccentricity of the pre-trim orbit

ψ_4 inclination of the pre-trim orbit

ψ_5 ascending node of the pre-trim orbit

Table VII -3 compares constraint vector errors computed from linearly-propagated errors with errors propagated by "non-linear" means.

Table VII -3

Linear Propagation Verification: Constraint Parameters

$$PSI = \psi(\tilde{X}^+ + \varphi\tilde{x}_o + \begin{pmatrix} 0 \\ M\tilde{r} \end{pmatrix}) \text{ linear } \psi$$

$$ERR = XA - \psi(X^+) \qquad \text{linear } \psi \text{ error}$$

Sample		TRIMV	DRIFT	e	i	Ω
1	PSI	253.59	64.97	.057456	.659	151.932
	ERR	.06	.02	.000013	.000	- .008
2	PSI	284.83	66.78	.045527	1.117	136.212
	ERR	.06	.02	.000020	.000	- .003
3	PSI	317.76	68.99	.041745	1.616	130.577
	ERR	.07	.02	.000026	.000	- .001
4	PSI	252.05	64.81	.058739	.645	153.628
	ERR	.13	.04	.000027	.000	- .020
5	PSI	283.13	66.59	.046765	1.097	136.928
	ERR	.13	.04	.000041	.000	- .006
6	PSI	315.89	68.77	.042661	1.592	130.961
	ERR	.14	.04	.000052	.000	- .002

Variation of some of these parameters with $\tilde{x}^+$ is very non-linear, so a Monte Carlo procedure was implemented as part of the error analysis algorithm. The valid assumption of linearity of error propagation from anchor epoch through the burn (equations (3), (13), and (18)) makes is reasonable to sample post-burn errors directly from P^+ of equation (19).

Statistical characteristics of the constraint parameter errors are computed from the Monte Carlo samples. These characteristics (as implemented to test the algorithm) are:

1. minimum value
2. maximum value
3. mean
4. standard deviation
5. probability that $|\tilde{\psi}| \leq \mathcal{E}$ ($\mathcal{E}$ input range)
6. probability that $|\tilde{\psi}| \leq 2\mathcal{E}$
7. probability that $|\tilde{\psi}| \leq 3\mathcal{E}$

A frequency histogram of 20 equal algorithm intervals about zero was also implemented for the test. All tests indicate that the algorithm as described is a valid one for error analysis of high thrust maneuvers.

The algorithm for error analysis of high-thrust maneuvers may thus be stated:

1. Propagate the navigation error covariance matrix to firing time (equation (5)).

2. Add the velocity-impulse error covariance matrix, M, to the navigation error covariance matrix at firing time (equation (19)).

3. Sample post-burn state errors from the resulting state error covariance matrix using a random number generator.

4. Add the sampled state errors to the errorless post-burn state.

5. Compute the mission constraint parameter error by differencing the value computed with the erroneous state and that computed with the errorless state.

6. Accumulate statistics of constraint parameter errors.

7. Return to step 3 a specified number of times.

8. Display statistics of constraint parameter errors.

APPENDIX A

This appendix consists of detailed tabular data pertaining to Section II on comet rendezvous missions. A glossary of the tabulated parameters precedes the tables, which have headings sufficient to define their contents.

The explanations and comments below may be helpful in clarifying the definitions and usefulness of some of the tabulated quantities. Refer also to the glossary mentioned in the preceding paragraph. These comments are in no particular order.

(1) The quantities r_{com} and θ_{com} may be used to determine (on all but the first table "Launch Date Variation") the rendezvous communication distance and angle along the orbit of the comet, i.e., after the rendezvous is accomplished and while the spacecraft is traveling along with the comet. Also, the p_t tabulation effectively displays the power available to the spacecraft as it moves along with the comet.

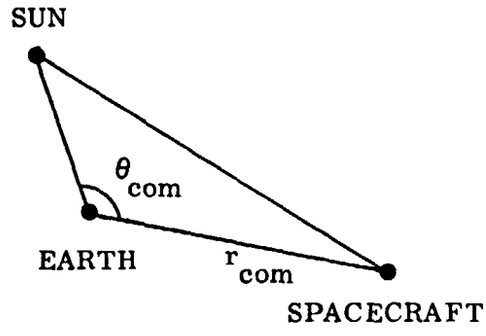

(2) The first table, labelled "Launch Date Variation", may be used to obtain a rough idea of the mission window width for the Giacobini-Zinner/1985 rendezvous mission using a Titan III E/Centaur launch vehicle; the results of a mission window analysis would depend on the analyst's criteria.

(3) In the burn time, t_b, tabulation, "cont." means "continuous" which stands for continuous thrusting throughout the pre-rendezvous portion of the mission: $t_b = t_f$. See the discussion in Section II of the main report concerned with single-engine throttling for the proper method of computing individual engine on-time requirements.

(4) Pertaining to ϕ_{min} and ϕ_{max}, the thrust cone angle ϕ is depicted by the following sketch:

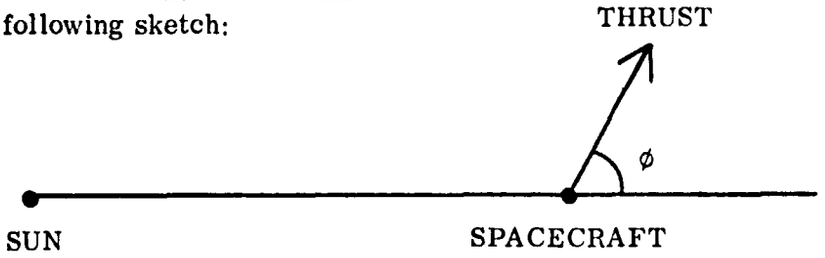

(5) The initial spacecraft mass is given by

$$m_o = m_{ps} + m_p + m_t + m_{net}$$

where m_{ps} is the propulsion system mass (see main text, Section II, for discussion), equal to 262.6 kilograms, m_p and m_{net} are tabulated, and $m_t = 0.1 \times m_p$. m_o was computed by the HILTOP program as a function of the launch characteristic speed v_c according to the expression:

$$m_o = b_1 e^{[-v_c/b_2]} - b_3$$

For m_o in kilograms and v_c in meters per second, the coefficients are:

	b_1	b_2	b_3
Titan III E/Centaur	167238.95	3480.2038	1753.6965
Shuttle/Transtage	2859382.94	1715.7632	1199.9231

(6) The importance of the launch asymptote declination δ and parking orbit inclination i are discussed in Section IV of the main text. When $|\delta| \leq 28^{o}.5$, the launch is due-east, and, for possible comparison with other studies, the tabulated m_o and v_∞ columns give the dependence of launch vehicle injected mass m_o on departure excess speed v_∞. This is not true when $|\delta| > 28^{o}.5$ because then other factors contribute to the launch phase characteristic speed.

GLOSSARY OF TABULATED PARAMETERS

AD	-	Arrival date, days from perihelion passage.
r_{min}	-	Minimum solar distance encountered along trajectory, AU.
r_{max}	-	Maximum solar distance encountered along trajectory, AU.
r_{com}	-	Earth-spacecraft distance at arrival, AU.
θ_{com}	-	Sun-Earth-spacecraft configuration angle at arrival, degrees.
ϕ_{min}	-	Minimum thrust cone angle required, degrees.
ϕ_{max}	-	Maximum thrust cone angle required, degrees.
$\Delta\lambda$	-	Change in longitude during the mission, degrees.
δ	-	Launch asymptote declination, degrees.
i	-	Inclination of launch parking orbit, degrees.
LD	-	Launch date, calendar date.
t_f	-	Mission duration, days.
t_b	-	Total propulsion system on time, days.
m_o	-	Initial spacecraft mass, kilograms.
m_p	-	Low thrust propellant mass, kilograms.
m_{net}	-	Net spacecraft mass, kilograms.
p_t	-	Power developed by arrays at target arrival, kilowatts.
v_∞	-	Launch hyperbolic excess speed, meters per second.

Giacobini-Zinner(85) Rendezvous — Titan III E/Centaur/Sert III — Launch Date Variation

AD	r_{min}	r_{max}	r_{com}	θ_{com}	ϕ_{min}	ϕ_{max}	$\Delta\lambda$	δ	i	LD	t_f	t_b	m_o	m_p	m_{net}	p_t	v_∞
0	.844	3.992	.45	79.6	50.9	159.3	470.7	44.27	32.50	6/8.5/81	1550	1394.?	1127.7	469.5	348.6	8.37	8053.7
0	.834	4.045	.45	79.6	49.5	163.7	461.2	38.44	32.50	6/18.5/81	1540	1406.9	1134.0	464.9	360.0	8.37	8619.6
0	.840	4.073	.45	79.6	46.1	166.7	451.6	31.67	30.98	6/28.5/81	1530	1417.7	1135.5	459.9	367.0	8.37	8813.5
0	.855	4.085	.45	79.6	41.1	166.1	442.1	23.93	28.50	7/8.5/81	1520	1424.1	1137.5	453.5	375.9	8.37	8829.7
0	.878	4.082	.45	79.6	35.2	160.2	432.5	15.10	28.50	7/18.5/81	1510	1430.2	1147.8	448.7	391.6	8.37	8809.8
0	.905	4.067	.45	79.6	29.2	151.0	423.0	5.24	28.50	7/28.5/81	1500	1433.7	1167.5	444.1	416.4	8.37	8772.0
0	.935	4.041	.45	79.6	24.0	139.6	413.4	-5.32	28.50	8/7.5/81	1490	1434.5	1198.8	439.7	452.6	8.37	8712.4
0	.964	4.011	.45	79.6	20.9	127.4	403.8	-15.26	28.50	8/17.5/81	1480	1432.6	1242.5	435.1	501.4	8.37	8629.6
0	.985	3.990	.45	79.6	20.3	116.0	394.2	-22.48	28.50	8/27.5/81	1470	1427.5	1295.1	429.5	560.0	8.37	8531.0
0	.996	3.984	.45	79.6	21.0	106.7	384.5	-26.17	28.50	9/6.5/81	1460	1418.9	1347.0	422.5	619.6	8.37	8434.7
0	1.001	3.992	.45	79.6	21.7	101.9	374.8	-27.16	28.50	9/16.5/81	1450	1407.3	1385.8	414.2	667.6	8.37	8363.3
0	1.001	4.008	.45	79.6	21.8	103.5	365.0	-26.42	28.50	9/26.5/81	1440	1393.6	1400.5	405.5	691.8	8.37	8336.5
0	1.000	4.026	.45	79.6	21.4	101.4	355.2	-24.50	28.50	10/6.5/81	1430	1379.6	1384.8	397.8	684.6	8.37	8365.3
0	.997	4.045	.45	79.6	20.4	99.3	345.3	-21.52	28.50	10/16.5/81	1420	1367.6	1339.1	391.7	645.6	8.37	8449.4
0	.994	4.065	.45	79.6	19.1	97.5	335.3	-17.32	28.50	10/26.5/81	1410	1358.1	1269.3	386.4	581.6	8.37	8579.3
0	.991	4.088	.45	79.6	17.7	96.1	325.3	-11.46	28.50	11/5.5/81	1400	1351.2	1185.5	381.1	503.7	8.37	8737.7
0	.989	4.114	.45	79.6	16.8	95.4	315.3	-3.75	28.50	11/15.5/81	1390	1348.4	1098.8	376.3	422.2	8.37	8904.5
0	.987	4.149	.45	79.6	16.8	96.0	305.2	5.04	28.50	11/25.5/81	1380	1353.9	1017.1	373.9	343.2	8.37	9064.5

Giacobini-Zinner(85) Rendezvous — **Titan III E/Centaur/Sert III** — **4-Year Missions**

AD	r_{min}	r_{max}	r_{com}	θ_{com}	ϕ_{min}	ϕ_{max}	$\Delta\lambda$	δ	i	LD	t_f	t_b	m_o	m_p	m_{net}	p_t	v_∞
0	1.001	4.013	.45	79.6	21.7	102.9	362.2	-26.00	28.50	9/29.3/81	1437.2	1389.6	1399.2	403.1	693.1	8.37	8338.8
-10	1.001	4.013	.47	80.0	23.0	105.8	351.6	-26.54	28.50	9/29.3/81	1427.2	1385.1	1384.3	396.2	685.9	8.26	8366.1
-20	1.001	4.017	.51	81.8	24.7	109.3	341.1	-27.07	28.50	9/29.2/81	1417.3	1383.2	1371.5	390.9	679.0	7.97	8389.6
-30	1.001	4.020	.57	84.3	26.7	113.4	331.0	-27.56	28.50	9/28.9/81	1407.6	1384.0	1361.2	387.4	672.4	7.53	8408.6
-40	1.000	4.022	.64	87.2	28.9	118.0	321.3	-27.98	28.50	9/28.5/81	1398.0	1387.9	1353.4	385.7	666.5	6.99	8423.0
-50	1.000	4.026	.71	90.1	30.5	122.4	312.2	-28.35	28.50	9/28.2/81	1388.3	cont.	1344.1	382.1	661.1	6.43	8440.2
-60	1.000	4.042	.79	92.8	29.8	126.9	302.7	-28.77	28.50	9/28.8/81	1377.7	cont.	1324.4	372.8	651.8	5.86	8476.1
-70	.998	4.067	.88	95.2	27.2	130.7	292.7	-29.13	28.50	9/30.8/81	1365.7	cont.	1294.7	362.9	632.9	5.33	8529.7
-80	.997	4.099	.98	96.9	23.5	134.1	283.1	-29.57	28.93	10/3.2/81	1353.3	cont.	1254.3	353.4	602.9	4.85	8602.2
-90	.995	4.133	1.08	98.0	19.5	137.1	274.3	-30.10	29.44	10/5.5/81	1341.0	cont.	1205.8	344.7	564.1	4.41	8690.1
-100	.994	4.167	1.19	98.2	15.7	139.6	266.6	-30.64	29.97	10/7.4/81	1329.1	cont.	1153.0	336.8	520.0	4.03	8787.1
-110	.991	4.201	1.32	97.6	12.1	141.8	259.9	-31.12	30.43	10/8.9/81	1317.6	cont.	1099.2	329.7	474.0	3.68	8887.7
-120	.989	4.234	1.45	96.0	9.0	143.6	254.2	-31.48	30.78	10/10.0/81	1306.5	cont.	1047.1	323.5	428.7	3.38	8987.1
-130	.985	4.265	1.60	93.7	6.1	145.2	249.4	-31.69	30.98	10/10.7/81	1295.8	cont.	996.8	318.0	384.4	3.12	9085.1
-140	.982	4.294	1.76	90.7	3.4	146.6	245.3	-31.71	30.99	10/11.0/81	1285.5	cont.	950.2	313.1	343.1	2.88	9178.2
-150	.978	4.321	1.93	87.0	0.9	147.8	241.9	-31.53	30.81	10/11.0/81	1275.5	cont.	907.0	309.0	304.6	2.67	9266.7

3-Year Missions

0	.999	3.135	.46	79.3	30.7	123.4	360.9	-34.88	32.50	10/1.4/82	1070.1	cont.	1336.7	434.4	596.3	8.37	8392.9
-10	.998	3.143	.48	79.8	32.6	127.0	350.8	-35.29	32.50	9/30.9/82	1060.6	cont.	1306.9	423.0	579.0	8.26	8436.9
-20	.996	3.159	.52	81.5	34.2	130.4	340.6	-35.65	32.50	9/30.5/82	1051.0	cont.	1272.4	411.7	557.0	7.97	8489.9
-30	.992	3.190	.57	84.0	34.0	133.6	329.9	-35.88	32.50	9/30.8/82	1040.7	cont.	1227.5	399.9	525.0	7.52	8567.2
-40	.985	3.235	.64	86.9	31.1	136.8	318.7	-35.87	32.50	10/1.9/82	1029.6	cont.	1167.9	387.9	478.6	6.99	8682.4
-50	.977	3.285	.72	89.8	26.7	139.7	308.2	-35.61	32.50	10/2.9/82	1018.6	cont.	1098.8	376.6	422.0	6.43	8826.1
-60	.967	3.333	.80	92.5	22.2	142.2	298.9	-35.11	32.50	10/3.4/82	1008.1	cont.	1028.0	366.4	362.3	5.86	8980.7
-70	.955	3.378	.89	94.8	18.1	144.4	291.1	-34.41	32.50	10/3.2/82	998.3	cont.	960.6	357.5	304.8	5.33	9131.5
-80	.943	3.420	.98	96.6	14.3	146.2	284.5	-33.55	32.50	10/2.4/82	989.0	cont.	898.6	349.7	251.4	4.85	9269.6

Giacobini-Zinner(85) Rendezvous — Shuttle/Transtage/Sert III — 4-Year Missions

AD	r_{min}	r_{max}	r_{com}	θ_{com}	ϕ_{min}	ϕ_{max}	$\Delta\lambda$	δ	i	LD	t_f	t_b	m_o	m_p	m_{net}	p_t	v_∞
0	1.004	3.992	.45	79.6	27.1	102.5	378.2	-5.94	28.50	9/13.0/81	1453.5	1361.4	1111.9	391.2	419.0	8.37	5271.4
-10	1.004	3.996	.47	80.0	28.0	104.8	366.9	-6.65	28.50	9/13.7/81	1442.8	1357.4	1102.8	385.7	415.9	8.26	5287.0
-20	1.004	4.000	.51	81.8	29.2	107.6	355.8	-7.33	28.50	9/14.2/81	1432.3	1354.9	1094.9	381.6	412.6	7.97	5300.5
-30	1.003	4.003	.57	84.3	30.5	110.9	345.0	-7.95	28.50	9/14.6/81	1421.9	1354.2	1088.3	378.6	409.2	7.53	5312.1
-40	1.003	4.007	.64	87.2	32.0	116.1	334.7	-8.51	28.50	9/14.8/81	1411.7	1355.4	1082.7	376.7	405.8	6.99	5321.6
-50	1.003	4.010	.71	90.1	33.6	121.4	325.1	-9.01	28.50	9/14.9/81	1401.6	1358.5	1078.3	375.7	402.4	6.43	5329.3
-60	1.003	4.013	.79	92.8	35.2	126.0	316.4	-9.44	28.50	9/14.8/81	1391.7	1363.8	1074.9	375.5	399.3	5.86	5335.2
-70	1.002	4.015	.88	95.2	36.9	129.5	308.6	-9.79	28.50	9/14.5/81	1382.0	1371.3	1072.7	376.0	396.5	5.33	5339.1
-80	1.002	4.026	.98	96.9	37.5	132.0	300.7	-10.06	28.50	9/15.2/81	1371.3	cont.	1066.3	372.7	393.6	4.85	5350.2
-90	1.001	4.054	1.08	98.0	35.6	133.2	291.5	-10.23	28.50	9/17.9/81	1358.6	cont.	1049.1	363.6	386.6	4.41	5379.8
-100	1.000	4.088	1.19	98.2	32.7	134.8	282.5	-10.47	28.50	9/21.2/81	1345.3	cont.	1026.4	354.5	373.8	4.03	5419.6
-110	.998	4.123	1.32	97.6	29.2	136.5	274.1	-10.88	28.50	9/24.5/81	1332.0	cont.	998.6	345.9	355.5	3.68	5468.1
-120	.997	4.160	1.45	96.0	25.5	138.4	266.4	-11.45	28.50	9/27.6/81	1318.9	cont.	967.2	337.9	332.9	3.38	5523.5
-130	.996	4.195	1.60	93.7	22.0	140.2	259.5	-12.13	28.50	9/30.4/81	1306.1	cont.	933.6	330.5	307.4	3.12	5583.1
-140	.994	4.230	1.76	90.7	18.8	141.9	253.4	-12.88	28.50	10/2.8/81	1293.7	cont.	899.1	323.7	280.4	2.88	5644.7
-150	.993	4.263	1.93	87.0	16.0	143.4	247.9	-13.63	28.50	10/4.9/81	1281.6	cont.	864.9	317.5	253.0	2.67	5706.3
-160	.991	4.294	2.10	82.9	13.5	144.8	243.2	-14.35	28.50	10/6.6/81	1269.9	cont.	831.6	312.0	225.9	2.49	5766.6
-170	.989	4.324	2.29	78.3	11.3	146.1	239.1	-15.02	28.50	10/7.9/81	1258.6	cont.	799.9	307.0	199.5	2.32	5824.7
-180	.987	4.352	2.47	73.5	9.4	147.3	235.5	-15.59	28.50	10/8.9/81	1247.6	cont.	769.8	302.6	174.3	2.18	5880.1
-190	.984	4.379	2.66	68.3	7.7	148.4	232.6	-16.06	28.50	10/9.5/81	1237.0	cont.	741.7	298.8	150.4	2.04	5932.4
-200	.981	4.404	2.85	62.9	6.1	149.4	230.2	-16.39	28.50	10/9.6/81	1226.9	cont.	715.5	295.5	127.8	1.93	5981.3
-210	.978	4.430	3.03	57.4	4.5	150.3	228.5	-16.56	28.50	10/9.3/81	1217.2	cont.	691.4	292.9	106.6	1.82	6026.7

Borrelly(87) Rendezvous — **Titan III E/Centaur/Sert III** — **4-Year Missions**

AD	r_{min}	r_{max}	r_{com}	θ_{com}	ϕ_{min}	ϕ_{max}	$\Delta\lambda$	δ	i	LD	t_f	t_b	m_o	m_p	m_{net}	p_t	v_∞
0	.978	4.026	.51	127.5	36.7	90.0	360.0	37.83	32.50	12/1.8/83	1477.7	cont.	1386.7	423.7	658.1	5.62	8167.1
-10	.978	4.029	.49	131.8	36.6	90.1	353.3	37.87	32.50	12/1.6/83	1467.9	cont.	1371.6	416.2	651.2	5.59	8192.9
-20	.978	4.031	.50	133.2	36.7	90.1	346.6	37.92	32.50	12/1.3/83	1458.2	cont.	1356.9	408.8	644.6	5.50	8218.0
-30	.977	4.034	.53	132.1	36.9	90.3	340.1	37.96	32.50	11/30.9/83	1448.6	cont.	1342.9	401.7	638.4	5.35	8242.0
-40	.977	4.036	.58	129.5	37.2	90.9	333.8	38.01	32.50	11/30.4/83	1439.1	cont.	1329.6	394.9	632.6	5.16	8264.9
-50	.976	4.039	.65	126.6	37.5	93.7	327.6	38.05	32.50	11/29.9/83	1429.6	cont.	1317.0	388.3	627.2	4.94	8286.6
-60	.976	4.042	.72	124.0	37.9	97.7	321.6	38.08	32.50	11/29.3/83	1420.2	cont.	1304.8	382.1	621.9	4.69	8307.9
-70	.975	4.046	.80	121.6	38.0	102.6	315.8	38.11	32.50	11/28.9/83	1410.6	cont.	1292.4	376.0	616.2	4.44	8329.9
-80	.975	4.052	.89	119.4	37.6	108.3	309.9	38.12	32.50	11/28.7/83	1400.8	cont.	1278.8	369.9	609.3	4.19	8355.6
-90	.974	4.062	.98	117.3	36.0	114.4	303.7	38.08	32.50	11/29.1/83	1390.4	cont.	1261.6	363.4	599.3	3.94	8391.5
-100	.974	4.079	1.08	115.1	32.8	119.8	296.8	37.95	32.50	11/30.5/83	1379.0	cont.	1238.1	356.4	583.5	3.70	8445.7
-110	.974	4.101	1.18	112.7	28.5	124.3	289.8	37.71	32.50	12/2.3/83	1367.2	cont.	1207.2	349.1	560.6	3.47	8520.1
-120	.974	4.126	1.29	110.1	24.0	128.0	282.9	37.39	32.50	12/4.3/83	1355.2	cont.	1170.2	342.1	531.3	3.26	8610.3
-130	.973	4.152	1.41	107.2	19.9	131.1	276.6	37.00	32.50	12/6.1/83	1343.4	cont.	1129.5	335.6	497.7	3.06	8710.3
-140	.972	4.178	1.54	104.0	16.4	133.6	270.8	36.55	32.50	12/7.6/83	1331.9	cont.	1087.0	329.6	461.8	2.88	8814.6
-150	.971	4.204	1.67	100.4	13.5	135.9	265.6	36.05	32.50	12/8.8/83	1320.7	cont.	1044.5	324.1	425.3	2.71	8919.7

3-Year Missions

0	.969	3.180	.51	128.0	40.5	102.3	360.8	38.87	32.50	11/30.2/84	1113.1	cont.	1286.0	425.6	555.3	5.62	8290.3
-10	.968	3.186	.49	132.3	41.5	105.8	354.4	38.84	32.50	11/29.7/84	1103.6	cont.	1265.0	418.0	542.6	5.59	8333.4
-20	.966	3.193	.50	133.6	42.5	110.0	348.0	38.79	32.50	11/29.2/84	1094.1	cont.	1242.5	410.5	528.4	5.50	8381.4
-30	.965	3.203	.53	132.3	43.3	114.9	341.6	38.68	32.50	11/28.7/84	1084.6	cont.	1217.3	402.9	511.5	5.35	8438.7
-40	.963	3.221	.58	129.6	43.6	120.4	334.8	38.43	32.50	11/28.6/84	1074.6	cont.	1186.6	394.9	489.6	5.16	8516.7
-50	.960	3.249	.65	126.6	42.3	125.9	327.1	37.87	32.50	11/29.6/84	1063.6	cont.	1146.5	385.9	459.5	4.94	8630.1
-60	.957	3.285	.72	123.9	39.9	130.5	318.9	37.00	32.50	12/1.2/84	1052.0	cont.	1097.3	376.5	420.6	4.69	8773.7
-70	.953	3.321	.80	121.5	37.0	134.3	311.2	35.90	32.50	12/2.6/84	1040.6	cont.	1043.7	367.7	376.6	4.44	8925.3
-80	.948	3.356	.89	119.3	34.2	137.4	304.3	34.68	32.50	12/3.4/84	1029.8	cont.	989.7	359.8	331.3	4.19	9067.8

Borrelly(87) Rendezvous **Shuttle/Transtage/Sert III** **4-Year Missions**

AD	r_{min}	r_{max}	r_{com}	θ_{com}	ϕ_{min}	ϕ_{max}	$\Delta\lambda$	δ	i	LD	t_f	t_b	m_o	m_p	m_{net}	p_t	v_∞
0	.986	3.959	.51	127.5	42.6	95.4	375.2	35.93	35.55	11/16.8/83	1492.7	1405.5	1131.5	401.8	426.9	5.62	5160.6
-10	.986	3.964	.49	131.8	42.8	95.6	367.8	36.25	35.86	11/17.2/83	1482.3	1398.4	1121.0	395.9	423.0	5.59	5175.1
-20	.986	3.968	.50	133.2	43.1	95.8	360.6	36.55	36.15	11/17.5/83	1472.0	1392.2	1111.3	390.5	419.2	5.50	5188.6
-30	.986	3.972	.53	132.1	43.5	97.9	353.4	36.81	36.41	11/17.8/83	1461.7	1387.2	1102.5	385.9	415.4	5.35	5201.0
-40	.986	3.977	.58	129.5	44.1	101.0	346.4	37.03	36.62	11/17.0/83	1451.5	1383.5	1094.6	382.0	411.8	5.16	5212.2
-50	.985	3.981	.65	126.6	44.8	104.4	339.5	37.20	36.80	11/18.1/83	1441.4	1381.3	1087.6	378.8	408.3	4.94	5222.2
-60	.985	3.985	.72	124.0	45.6	107.8	332.9	37.34	36.93	11/18.2/83	1431.3	1380.5	1081.6	376.4	405.0	4.70	5231.2
-70	.985	3.990	.80	121.6	46.4	111.2	326.6	37.44	37.03	11/18.2/83	1421.3	1381.3	1076.4	374.5	401.8	4.44	5239.1
-80	.985	3.994	.89	119.4	47.3	114.4	320.6	37.52	37.11	11/18.1/83	1411.4	1383.7	1072.0	373.3	398.8	4.19	5246.0
-90	.984	3.998	.98	117.3	48.2	117.5	314.9	37.57	37.16	11/17.0/83	1401.6	1387.8	1068.4	372.5	396.0	3.94	5251.6
-100	.984	4.003	1.08	115.1	49.1	120.7	309.6	37.61	37.20	11/17.8/83	1391.7	cont.	1064.8	371.6	393.4	3.70	5257.5
-110	.984	4.017	1.18	112.7	48.7	124.0	303.8	37.38	36.97	11/18.4/83	1381.1	cont.	1054.6	365.7	389.8	3.48	5278.2
-120	.983	4.039	1.29	110.1	47.3	126.3	297.3	36.70	36.29	11/20.1/83	1369.4	cont.	1040.8	359.0	383.3	3.26	5310.6
-130	.983	4.068	1.41	107.2	44.7	128.3	290.3	35.69	35.28	11/22.5/83	1357.0	cont.	1022.3	351.9	372.6	3.06	5354.8
-140	.982	4.100	1.54	104.0	41.3	130.2	283.4	34.54	34.14	11/25.2/83	1344.3	cont.	999.4	344.8	357.6	2.88	5407.9
-150	.981	4.131	1.67	100.4	37.6	132.1	276.7	33.37	32.98	11/27.9/83	1331.6	cont.	973.1	337.9	338.8	2.71	5467.0
-160	.981	4.163	1.82	96.6	33.9	133.9	270.5	32.21	31.82	11/30.4/83	1319.1	cont.	944.6	331.5	317.3	2.56	5529.7
-170	.980	4.192	1.97	92.6	30.3	135.7	264.9	31.06	30.67	12/2.5/83	1307.9	cont.	914.8	325.5	294.1	2.41	5594.3
-180	.979	4.221	2.12	88.3	27.1	137.3	259.8	29.90	29.51	12/4.4/83	1295.1	cont.	881.8	320.0	270.2	2.28	5659.3
-190	.978	4.248	2.28	83.8	24.1	138.8	255.2	28.86	28.50	12/6.0/83	1283.5	cont.	855.2	315.0	246.1	2.16	5722.3
-200	.977	4.273	2.45	79.1	21.8	140.3	251.0	28.74	28.50	12/7.4/83	1272.1	cont.	826.2	310.3	222.3	2.05	5775.8
-210	.976	4.298	2.62	74.3	19.7	141.7	247.2	28.61	28.50	12/8.5/83	1261.0	cont.	798.3	306.1	199.0	1.95	5827.4

Tempel II(88) Rendezvous — **Titan III E/Centaur/Sert III** — **4-Year Missions**

AD	r_{min}	r_{max}	r_{com}	θ_{com}	ϕ_{min}	ϕ_{max}	$\Delta\lambda$	δ	i	LD	t_f	t_b	m_o	m_p	m_{net}	p_t	v_∞
0	1.016	3.919	.96	89.4	64.1	98.0	371.0	-5.39	28.50	7/21.5/84	1518.0	1387.1	2361.7	395.9	1663.6	5.45	6690.9
-10	1.015	3.923	.92	91.9	64.1	99.2	363.1	-5.53	28.50	7/22.1/84	1507.4	1387.3	2353.1	391.9	1659.5	5.42	6704.9
-20	1.015	3.927	.89	94.9	64.1	100.7	355.3	-5.68	28.50	7/22.7/84	1496.8	1388.2	2344.1	388.1	1654.6	5.35	6719.6
-30	1.015	3.931	.86	98.6	64.1	102.6	347.6	-5.82	28.50	7/23.3/84	1486.2	1390.1	2334.8	384.7	1649.1	5.23	6734.8
-40	1.015	3.936	.83	103.0	64.1	104.8	340.2	-5.94	28.50	7/23.8/84	1475.7	1393.2	2325.3	381.6	1642.9	5.08	6750.3
-50	1.015	3.941	.81	108.2	64.1	107.3	333.1	-6.04	28.50	7/24.3/84	1465.2	1398.1	2315.8	379.0	1636.3	4.89	6765.9
-60	1.015	3.946	.79	114.3	64.1	110.0	326.4	-6.10	28.50	7/24.9/84	1454.6	1405.2	2306.3	376.8	1629.2	4.69	6781.3
-70	1.015	3.952	.78	121.2	64.2	112.8	319.9	-6.11	28.50	7/25.4/84	1444.1	1415.2	2297.1	375.3	1621.7	4.47	6796.4
-80																	
-90	1.015	3.963	.78	137.3	64.5	119.5	308.3	-6.37	28.50	7/26.0/84	1423.5	cont.	2274.2	369.4	1605.3	4.03	6834.0
-100	1.015	3.968	.79	145.5	64.8	123.1	303.2	-6.73	28.50	7/26.1/84	1413.4	cont.	2257.5	363.7	1594.8	3.81	6861.4
-110	1.014	3.976	.83	152.4	65.1	126.4	298.3	-7.07	28.50	7/26.3/84	1403.2	cont.	2238.1	358.3	1581.4	3.60	6893.2
-120	1.014	3.987	.88	156.1	65.0	129.4	293.6	-7.43	28.50	7/26.6/84	1392.9	cont.	2213.7	352.9	1562.9	3.40	6933.4
-130	1.014	4.003	.95	155.0	64.2	131.6	288.8	-7.87	28.50	7/27.3/84	1382.2	cont.	2180.0	347.4	1535.3	3.22	6988.9
-140	1.014	4.025	1.04	149.8	61.7	133.3	283.9	-8.51	28.50	7/28.4/84	1371.1	cont.	2131.3	341.6	1492.9	3.04	7069.5
-150	1.013	4.045	1.14	142.7	57.7	135.0	279.0	-9.26	28.50	7/29.6/84	1359.9	cont.	2068.7	336.0	1436.6	2.88	7173.7
-160	1.013	4.063	1.27	134.9	52.8	136.7	274.5	-9.91	28.50	7/30.8/84	1348.7	cont.	1993.2	330.6	1366.9	2.75	7300.2
-170	1.012	4.079	1.41	127.1	48.1	138.4	270.6	-10.28	28.50	7/31.5/84	1338.0	cont.	1916.3	326.0	1295.2	2.59	7430.1
-180	1.010	4.093	1.56	119.4	43.6	140.0	267.2	-10.38	28.50	7/31.8/84	1327.7	cont.	1840.0	321.8	1223.4	2.46	7560.2
-190	1.009	4.106	1.73	111.9	39.2	141.7	264.3	-10.24	28.50	7/31.9/84	1317.6	cont.	1766.0	318.2	1153.5	2.34	7687.3
-200	1.007	4.118	1.90	104.7	35.0	143.4	261.8	-9.91	28.50	7/31.6/84	1307.9	cont.	1695.5	314.9	1086.5	2.23	7809.9

Tempel II(88) Rendezvous **Titan III E/Centaur/Sert III** **3-Year Missions**

AD	r_{min}	r_{max}	r_{com}	θ_{com}	ϕ_{min}	ϕ_{max}	$\Delta\lambda$	δ	i	LD	t_f	t_b	m_o	m_p	m_{net}	p_t	v_∞
0	1.010	3.168	.96	89.4	70.1	131.3	363.4	-15.53	28.50	7/29.7/85	1144.8	cont.	2272.7	428.3	1539.0	5.45	6836.4
-10	1.007	3.191	.92	91.9	67.1	134.0	355.1	-15.07	28.50	7/30.7/85	1133.8	cont.	2172.3	419.2	1448.6	5.43	7001.6
-20	1.004	3.212	.89	94.9	63.1	136.7	347.4	-14.19	28.50	7/31.2/85	1123.3	cont.	2063.1	410.6	1348.8	5.35	7183.1
-30	1.000	3.233	.86	98.6	58.4	139.3	340.3	-12.92	28.50	7/31.2/85	1113.3	cont.	1952.0	402.8	1246.3	5.23	7369.7
-40	.994	3.253	.83	103.0	53.4	141.8	333.9	-11.36	28.50	7/30.7/85	1103.8	cont.	1843.0	395.8	1145.1	5.08	7554.9
-60	.980	3.292	.79	114.3	48.3	145.7	324.2	-7.68	28.50	7/27.4/85	1087.1	1069.1	1626.9	372.7	954.3	4.69	7930.2
-70	.971	3.311	.78	121.2	46.1	147.2	320.6	-5.89	28.50	7/24.9/85	1079.6	1051.2	1527.9	362.0	867.1	4.47	8105.9
-80	.961	3.331	.77	129.0	43.3	148.3	317.8	-4.13	28.50	7/21.8/85	1072.7	1035.2	1437.3	353.6	785.7	4.25	8269.4
-90	.949	3.352	.78	137.3	40.2	148.9	316.2	-2.33	28.50	7/17.0/85	1066.5	1021.0	1355.3	347.5	710.5	4.02	8419.5
-100	.934	3.373	.79	145.5	37.0	148.8	316.0	-0.30	28.50	7/12.9/85	1061.6	1009.4	1282.5	344.2	641.2	3.81	8554.6
-110	.915	3.395	.83	152.4	34.1	147.5	318.4	2.38	28.50	7/5.5/85	1059.6	1003.1	1221.4	346.2	578.0	3.60	8669.6

2-Year Missions

0	.825	2.435	.88	89.4	54.0	128.8	414.2	7.14	28.50	6/6.7/86	822.8	cont.	1346.8	462.8	575.2	5.45	8435.1
-10	.792	2.465	.92	91.9	57.5	128.7	416.6	9.21	28.50	5/27.6/86	832.9	cont.	1287.9	459.7	519.6	5.43	8544.6
-20	.761	2.497	.89	94.9	58.9	129.9	417.5	10.27	28.50	5/19.1/86	831.4	cont.	1288.9	454.7	466.2	5.35	8655.3
-30	.731	2.531	.86	98.6	59.0	169.0	417.6	10.75	28.50	5/11.6/86	828.9	cont.	1171.0	448.5	415.1	5.23	8765.4
-40	.701	2.566	.83	103.0	58.3	168.3	417.3	10.89	28.50	5/4.8/86	825.7	cont.	1114.7	441.5	366.5	5.08	8873.6
-50	.671	2.602	.81	108.2	57.3	167.7	416.8	10.85	28.50	4/28.5/86	822.0	cont.	1060.6	434.0	320.5	4.89	8979.0
-60	.642	2.639	.79	114.3	56.0	167.3	416.2	10.73	28.50	4/22.6/86	817.9	cont.	1008.9	426.2	277.5	4.69	9080.7
-70	.612	2.676	.78	121.2	54.7	166.9	415.6	10.58	28.50	4/17.2/86	813.3	cont.	959.9	418.7	237.3	4.47	9178.4
-80	.583	2.714	.77	129.0	53.4	166.6	415.0	10.43	28.50	4/12.1/86	808.4	cont.	913.6	410.0	200.0	4.25	9271.6
-90	.555	2.751	.78	137.3	52.1	166.3	414.3	10.32	28.50	4/7.3/86	803.2	cont.	870.1	401.8	165.5	4.02	9360.3
-100	.527	2.788	.79	145.5	50.9	166.1	413.7	10.26	28.50	4/2.9/86	797.6	cont.	829.4	393.7	133.6	3.81	9444.2

Tempel II(88) Rendezvous | **Shuttle/Transtago/Sert III** | **4-Year Missions**

AD	r_{min}	r_{max}	r_{com}	θ_{com}	ϕ_{min}	ϕ_{max}	$\Delta\lambda$	δ	i	LD	t_f	t_b	m_o	m_p	m_{net}	p_t	v_∞
0	1.016	3.768	.96	89.4	50.2	104.2	400.3	-3.51	28.50	6/20.7/84	1548.8	1139.3	1436.1	343.2	796.1	5.45	4726.0
-20	1.016	3.777	.89	94.9	50.1	109.9	383.9	-2.88	28.50	6/22.7/84	152€.8	1141.3	1433.1	342.3	794.0	5.35	4731.1
-40	1.016	3.789	.83	103.0	50.0	115.9	368.0	-2.32	28.50	6/24.7/84	1504.8	1144.9	1428.5	341.4	790.4	5.08	4738.7
-60	1.016	3.803	.79	114.3	50.0	122.1	353.2	-1.82	28.50	6/26.7/84	1482.8	1149.9	1422.6	340.4	785.6	4.69	4748.4
-80	1.016	3.819	.77	129.0	49.9	128.4	339.7	-1.37	28.50	6/28.7/84	1460.8	1156.7	1415.7	339.6	779.6	4.25	4759.8
-100	1.016	3.836	.79	145.5	49.9	134.5	327.5	-.95	28.50	6/30.6/84	1438.9	1165.8	1407.9	338.9	772.5	3.81	4772.7
-120	1.016	3.855	.88	156.1	49.9	139.9	316.6	-.52	28.50	7/2.5/84	1417.0	1179.1	1399.4	338.5	764.4	3.40	4786.9
-140	1.016	3.877	1.04	149.8	49.8	143.8	306.9	-.04	28.50	7/4.3/84	1395.2	1198.5	1390.1	338.4	755.3	3.04	4802.3
-160	1.016	3.902	1.27	134.9	49.7	146.9	298.1	.57	28.50	7/6.1/84	1373.4	1227.6	1380.0	338.7	744.8	2.73	4818.9
-180	1.016	3.932	1.56	119.4	49.4	150.2	290.0	1.42	28.50	7/8.0/84	1351.5	1272.2	1369.2	339.9	732.7	2.46	4837.0
-200	1.015	3.975	1.90	104.7	48.4	152.9	282.2	2.76	28.50	7/10.2/84	1329.3	cont.	1355.6	340.8	718.1	2.23	4859.6
-220	1.015	4.032	2.27	90.6	45.6	149.3	273.2	4.20	28.50	7/14.3/84	1305.2	cont.	1322.0	330.5	695.8	2.03	4915.6
-240	1.014	4.084	2.64	77.1	41.2	146.9	264.5	5.30	28.50	7/18.7/84	1280.8	cont.	1275.4	320.4	660.3	1.86	4993.6
-260	1.014	4.126	3.01	63.9	35.9	146.4	256.7	5.64	28.50	7/22.6/84	1256.9	cont.	1217.3	311.1	612.5	1.72	5091.6
-280	1.012	4.159	3.35	51.0	30.6	147.2	249.9	5.47	28.50	7/25.6/84	1233.9	cont.	1153.6	302.9	557.8	1.59	5199.9
-300	1.011	4.186	3.66	38.4	26.1	148.7	244.3	5.19	28.50	7/27.8/84	1211.7	cont.	1089.6	295.9	501.4	1.48	5309.8
-320	1.009	4.211	3.92	26.1	22.3	150.4	239.8	5.01	28.50	7/29.2/84	1190.3	cont.	1028.2	290.1	446.5	1.38	5416.3

Tempel II(88) Rendezvous **Shuttle/Transtage/Sert III** **3-Year Missions**

AD	r_{min}	r_{max}	r_{com}	θ_{com}	ϕ_{min}	ϕ_{max}	$\Delta\lambda$	δ	i	LD	t_f	t_b	m_o	m_p	m_{net}	p_t	v_∞
0	1.016	3.028	.96	89.4	57.9	128.0	382.2	-3.75	28.50	7/9.0/85	1164.5	1021.5	1633.8	413.2	916.7	5.45	4401.8
-10	1.016	3.044	.92	91.9	58.0	132.4	372.6	-3.42	28.50	7/12.4/85	1152.1	1029.8	1619.4	410.8	904.9	5.40	4425.2
-20	1.015	3.062	.89	94.9	58.1	136.6	363.0	-3.04	28.50	7/14.8/85	1139.7	1042.8	1603.1	409.0	890.6	5.35	4451.9
-30	1.015	3.082	.86	98.6	58.3	140.8	353.6	-2.54	28.50	7/17.3/85	1127.2	1063.0	1585.0	407.8	873.8	5.23	4481.4
-40	1.015	3.108	.83	103.0	58.5	145.9	344.3	-1.72	28.50	7/19.9/85	1114.6	1098.4	1565.0	408.6	853.0	5.08	4514.1
-50	1.014	3.142	.81	108.2	58.6	147.4	334.7	-1.15	28.50	7/22.0/85	1101.5	cont.	1531.2	401.3	827.2	4.89	4559.6
-60	1.013	3.180	.79	114.3	58.2	147.4	325.0	-0.53	28.50	7/26.5/85	1088.0	cont.	1484.4	390.5	792.3	4.69	4616.6
-70	1.012	3.221	.78	121.2	57.2	147.4	315.4	0.34	28.50	7/30.3/85	1074.2	cont.	1425.6	379.6	746.4	4.47	4741.8
-80	1.011	3.256	.77	129.0	55.5	147.8	306.5	1.23	28.50	8/2.7/85	1060.8	cont.	1362.7	369.5	693.6	4.25	4847.8
-90	1.009	3.288	.78	137.3	53.4	148.8	298.5	2.02	28.50	8/5.5/85	1048.0	cont.	1295.0	360.3	636.1	4.02	4960.6
-100	1.006	3.316	.79	145.5	51.1	150.2	291.7	2.73	28.50	8/7.4/85	1036.1	cont.	1228.3	352.4	578.1	3.81	5073.0
-110	1.003	3.341	.83	152.5	48.8	151.8	286.1	3.39	28.50	8/8.3/85	1025.2	cont.	1161.8	345.8	521.8	3.60	5180.8
-120	1.000	3.364	.88	156.1	46.4	153.4	281.9	4.08	28.50	8/8.1/85	1015.4	cont.	1095.7	340.7	468.3	3.40	5282.0
-130	.994	3.386	.95	155.0	43.8	155.0	279.3	4.82	28.50	8/6.4/85	1007.1	cont.	1052.3	337.5	418.5	3.22	5374.3
-140	.986	3.409	1.04	149.8	40.5	156.4	279.7	5.72	28.50	8/2.0/85	1001.5	cont.	1005.7	337.5	371.9	3.04	5456.7

2-Year Missions

100	1.012	2.201	1.83	68.1	66.2	129.4	435.6	-19.73	28.50	7/21.6/86	887.9	cont.	1811.1	511.1	986.2	3.81	4112.8
90	1.011	2.211	1.71	71.1	66.1	130.9	429.2	-19.22	28.50	7/23.0/86	876.5	cont.	1773.9	503.7	957.3	4.02	4173.4
80	1.009	2.222	1.59	75.9	65.9	132.6	422.5	-18.51	28.50	7/24.3/86	865.2	cont.	1732.3	496.0	924.1	4.25	4241.2
70	1.007	2.235	1.48	76.3	65.6	134.3	415.7	-17.53	28.50	7/25.4/86	854.1	cont.	1686.2	488.2	886.6	4.47	4316.3
60	1.004	2.249	1.37	78.5	64.9	136.2	408.9	-16.42	28.50	7/26.2/86	843.3	cont.	1635.8	480.4	844.7	4.68	4398.5
50	1.000	2.265	1.28	80.4	64.0	138.1	402.2	-15.00	28.50	7/26.5/86	833.0	cont.	1581.4	472.8	798.8	4.89	4487.3
40	.995	2.282	1.20	82.2	62.7	140.1	395.6	-13.40	28.50	7/26.4/86	823.1	cont.	1523.4	465.2	749.0	5.08	4582.3
30	.988	2.300	1.12	83.8	60.9	142.0	389.8	-11.48	28.50	7/25.1/86	811.4	cont.	1463.0	458.6	695.9	5.23	4681.7
20	.979	2.320	1.06	85.5	58.4	143.7	385.3	-9.23	28.50	7/22.3/86	807.1	cont.	1401.5	453.2	640.4	5.35	4784.3
10	.966	2.342	1.01	87.3	55.0	144.7	383.3	-6.54	28.50	7/16.8/86	802.7	cont.	1341.2	450.2	583.4	5.43	4888.5
0	.945	2.368	.96	89.4	51.1	144.2	386.3	-3.11	28.50	7/5.9/86	803.6	cont.	1285.8	451.9	526.2	5.45	4990.1
-10	.910	2.397	.92	91.9	49.4	141.7	396.6	0.98	28.50	6/17.5/86	812.0	cont.	1238.9	459.7	470.8	5.43	5085.0
-20	.869	2.432	.89	94.9	50.9	140.1	408.0	3.98	28.50	5/28.0/86	821.5	cont.	1193.6	466.0	418.4	5.35	5171.7

Tempel II(83) Rendezvous **Titan III E/Centaur/Sert III** **2-Year Missions**

AD	r_{min}	r_{max}	r_{com}	θ_{com}	ϕ_{min}	ϕ_{max}	$\Delta\lambda$	δ	i	LD	t_f	t_b	m_o	m_p	m_{net}	p_t	v_∞
250	.982	2.001	2.59	83.4	68.9	146.7	487.2	-21.97	28.50	7/17.6/81	933.9	842.4	1918.5	488.5	1118.6	1.79	7426.3
240	.981	1.999	2.40	90.6	69.5	146.7	485.3	-21.61	28.50	7/17.3/81	924.2	832.0	1902.1	485.1	1105.9	1.86	7454.2
230	.979	1.997	2.21	98.1	70.1	146.5	483.4	-21.22	28.50	7/17.1/81	914.4	821.7	1884.9	481.7	1092.5	1.94	7483.4
220	.977	1.995	2.03	105.8	70.6	146.4	481.3	-20.79	28.50	7/16.8/81	904.7	811.5	1867.0	478.3	1078.3	2.03	7513.9
210	.974	1.994	1.85	113.8	71.2	146.1	479.2	-20.32	28.50	7/16.5/81	895.0	801.5	1848.3	474.8	1063.4	2.13	7545.9
200	.972	1.993	1.68	122.2	71.6	145.8	476.9	-19.81	28.50	7/16.2/81	885.3	791.7	1828.7	471.4	1047.6	2.23	7579.4
190	.969	1.992	1.52	130.7	72.1	145.4	474.6	-19.25	28.50	7/15.8/81	875.7	782.1	1808.2	468.0	1030.8	2.34	7614.7
180	.996	1.992	1.39	139.4	72.5	144.9	472.1	-18.65	28.50	7/15.6/81	866.1	772.8	1786.6	464.6	1012.9	2.46	7651.8
170	.963	1.993	1.26	147.6	75.3	144.3	469.5	-17.98	28.50	7/14.9/81	856.6	763.8	1763.9	461.3	993.9	2.59	7691.0
160	.959	1.994	1.16	154.0	73.0	143.6	466.7	-17.26	28.50	7/14.4/81	847.1	755.0	1739.9	458.0	973.6	2.73	7732.5
150	.955	1.996	1.09	156.3	73.2	142.7	463.9	-16.48	28.50	7/13.8/81	837.7	746.6	1714.6	454.7	951.8	2.88	7776.5
140	.950	1.998	1.03	153.0	73.2	141.6	460.9	-15.62	28.50	7/13.1/81	828.4	738.7	1687.9	451.6	928.5	3.05	7823.1
130	.945	2.001	1.00	145.7	73.2	140.4	457.7	-14.69	28.50	7/12.3/81	819.2	731.1	1659.5	448.5	903.5	3.22	7872.8
120	.939	2.006	0.99	136.8	72.9	139.0	454.5	-13.68	28.50	7/11.3/81	810.2	724.0	1629.4	445.6	876.6	3.41	7925.7
110	.932	2.012	0.99	127.8	72.5	137.6	451.1	-12.57	28.50	7/10.1/81	801.4	717.6	1597.5	442.9	847.7	3.60	7982.1
100	.924	2.019	1.00	119.2	72.0	136.0	447.7	-11.35	28.50	7/8.7/81	792.8	711.7	1563.7	440.3	816.7	3.81	8042.1
90	.915	2.027	1.01	111.4	71.2	134.5	444.2	-10.00	28.50	7/7.0/81	784.4	706.7	1527.8	438.1	783.3	4.03	8106.1
80	.905	2.038	1.03	104.5	70.2	133.0	440.8	-8.49	28.50	7/4.9/81	776.5	702.8	1490.1	436.3	747.6	4.25	8173.8
70	.893	2.050	1.05	98.5	69.0	131.5	437.6	-6.76	28.50	7/2.3/81	769.2	700.3	1450.8	435.2	709.4	4.47	8244.9
60	.878	2.065	1.08	93.3	67.5	130.0	434.8	-4.75	28.50	6/28.8/81	762.6	699.9	1410.4	435.3	668.9	4.69	8318.4
50	.860	2.083	1.10	88.8	65.8	128.3	432.9	-2.28	28.50	6/24.1/81	757.4	703.2	1370.4	437.7	626.3	4.90	8391.6
40	.836	2.106	1.12	85.1	64.0	126.4	433.0	1.00	28.50	6/16.9/81	754.6	714.2	1334.8	445.7	581.9	5.09	8457.2
30	.790	2.140	1.14	81.9	65.1	121.9	444.6	7.76	28.50	5/28.5/81	764.0	cont.	1336.0	487.6	537.0	5.24	8455.1
20	.761	2.170	1.17	79.3	67.4	121.8	445.1	9.57	28.50	5/20.5/81	762.0	cont.	1286.0	482.2	493.0	5.36	8548.0
10	.731	2.201	1.20	77.1	68.2	122.6	444.4	10.69	28.50	5/13.6/81	758.9	cont.	1234.1	475.2	448.8	5.44	8645.5
0	.701	2.235	1.23	75.3	67.9	166.8	443.0	11.30	28.50	5/7.5/81	755.0	cont.	1181.0	467.1	404.6	5.47	8746.2
-10	.672	2.270	1.27	73.8	66.9	165.2	441.0	11.58	28.50	5/1.9/81	750.6	cont.	1127.4	458.1	360.8	5.44	8849.1
-20	.642	2.306	1.32	72.5	65.4	163.9	438.9	11.66	28.50	4/26.7/81	745.8	cont.	1074.0	448.8	317.8	5.36	8952.7
-30	.612	2.343	1.38	71.2	63.7	162.8	436.6	11.63	28.50	4/21.7/81	740.8	cont.	1021.4	439.0	275.8	5.24	9056.0
-40	.583	2.381	1.44	69.8	61.9	161.9	434.4	11.56	28.50	4/16.9/81	735.6	cont.	970.2	429.1	235.5	5.09	9157.8
-50	.553	2.420	1.52	68.4	60.1	161.2	432.2	11.51	28.50	4/12.4/81	730.1	cont.	920.8	419.2	197.1	4.90	9257.1
-60	.524	2.459	1.61	66.7	58.4	160.7	430.2	11.49	28.50	4/8.1/81	724.4	cont.	873.7	409.4	160.8	4.69	9352.9
-70	.496	2.498	1.71	64.8	56.7	160.3	428.2	11.54	28.50	4/3.9/81	718.5	cont.	829.1	399.6	126.9	4.47	9444.9

APPENDIX B

The equations for the partial derivatives $\partial v_g/\partial v_\infty$ and $\partial v_g/\partial \delta$ are derived from Equations (5) and (6) of Section IV and are listed below:

$$\frac{\partial v_g}{\partial v_\infty} = \frac{v_o^2}{v_g}\left\{\rho\frac{\partial \rho}{\partial v_\infty} - \frac{w(3+2\rho w - w^2)(\partial\rho/\partial v_\infty) + (3\rho + 2\rho^2 w - 3\rho w^2 - 4w)(\partial w/\partial v_\infty)}{2\sqrt{(1+\rho w - w^2)(2+\rho w)}}\right\},$$

$$\frac{\partial v_g}{\partial \delta} = -\frac{v_o^2(3\rho + 2\rho^2 w - 3\rho w^2 - 4w)}{2v_g\sqrt{(1+\rho w - w^2)(2+\rho w)}}\ \frac{\partial w}{\partial \delta},$$

where

$$\partial\rho/\partial v_\infty = 1/v_o,$$

$$\frac{\partial w}{\partial v_\infty} = \frac{1}{2}\left\{\frac{1}{2}\frac{\partial \rho}{\partial v_\infty} + \frac{\partial y}{\partial v_\infty} + \left[\left(1 + \frac{x}{2\sqrt{x^2/4 + s^2}}\right)\frac{\partial x}{\partial v_\infty} + \left(\frac{\rho}{2} + y\right)\left(\frac{1}{2}\frac{\partial \rho}{\partial v_\infty} + \frac{\partial y}{\partial v_\infty}\right)\right]/(2w - \rho/2 - y)\right\},$$

$$\frac{\partial w}{\partial \delta} = \frac{1}{2}\left\{\frac{\partial y}{\partial \delta} + \left[\frac{\partial x}{\partial \delta} + \frac{x(\partial x/\partial\delta) + 4s(\partial s/\partial\delta)}{2\sqrt{x^2/4 + s^2}} + \left(\frac{\rho}{2} + y\right)\frac{\partial y}{\partial \delta}\right]/(2w - \rho/2 - y)\right\},$$

$$\partial s/\partial\delta = \cos(\delta - i),$$

$$\partial y/\partial v_\infty = \left[(\rho/2)\,\partial\rho/\partial v_\infty - \partial x/\partial v_\infty\right]/2y,$$

$$\partial y/\partial\delta = -(\partial x/\partial\delta)/2y,$$

$$\frac{\partial x}{\partial u} = \frac{1}{6}\left[\frac{(q/2)(\partial q/\partial u) + (p/3)^2(\partial p/\partial u)}{\sqrt{(q/2)^2 + (p/3)^3}} + \frac{\partial q}{\partial u}\right]\left[\sqrt{(q/2)^2 + (p/3)^3} + q/2\right]^{-2/3}$$

$$-\frac{1}{6}\left[\frac{(q/2)(\partial q/\partial u) + (p/3)^2(\partial p/\partial u)}{\sqrt{(q/2)^2 + (p/3)^3}} - \frac{\partial q}{\partial u}\right]\left[\sqrt{(q/2)^2 + (p/3)^3} - q/2\right]^{-2/3}$$

with $u = v_\infty$ or δ,

$$\partial q/\partial v_\infty = 2\rho s^2(1 - s^2)(\partial \rho/\partial v_\infty),$$

$$\partial q/\partial \delta = 2\rho^2 s(1 - 2s^2)(\partial s/\partial \delta),$$

$$\partial p/\partial v_\infty = 2\rho s^2(\partial \rho/\partial v_\infty),$$

$$\partial p/\partial \delta = 2s(\rho^2 + 4)(\partial s/\partial \delta).$$

REFERENCES

[1] F. I. Mann, J. L. Horsewood and P. F. Flanagan, "HILTOP, Heliocentric Interplanetary Low Thrust Trajectory Optimization Program," AMA, Inc. Report No. 73-1, January 1973.

[2] Private Communication, Mr. Robert C. Finke of NASA Lewis Research Center to Dr. Robert W. Farquhar of NASA Goddard Space Flight Center, October 10, 1973; also, Telecon, Mr. Robert C. Finke to Mr. J. L. Horsewood of AMA, Inc., December 21, 1973.

[3] "Launch Vehicles Estimating Factors," NASA Office of Space Science, 1973 Edition.

[4] P. Gunther, "Asymptotically Optimum Two-Impulse Transfer from Lunar Orbit," AIAA Journal, Vol. 4, No. 2, pp. 346-349, February 1966.

[5] F. I. Mann and J. L. Horsewood, "Selected Solar Electric Propulsion and Ballistic Missions Studies," NASA CR-132753, January 1973.

[6] A. C. Mascy, R. W. Schaupp and S. A. Hayes, "QUICKTOP III - A Computer Program for Low-Thrust Trajectory and Mass Optimization," NASA TM X-62,305, September 1973.

[7] F. T. Johnson, "Improvement of the QUICKTOP Digital Computer Program (CHEBYTOP III)," NASA CR-114595, April 1973.

[8] J. L. Horsewood, F. I. Mann and K. B. Brice, "The Generation and Interpretation of Electric Propulsion Mission Analysis Data," AMA, Inc. Report No. 73-38, August 1973.

[9] J. L. Horsewood and F.I. Mann, "The Optimizatic Low Thrust Heliocentric Trajectories with Large Launch Asymptote Declinations," AIAA Paper No. 74-803, Presented at the AIAA Mechanics and Control of Flight Conference, Anaheim, California, August 5-9, 1974.

[10] F.I. Mann and J. L. Horsewood, "HILTOP Supplement, Heliocentric Interplanetary Low Thrust Trajectory Optimization Program," Supplement #1, AMA, Inc. Report No. 74-30, December 1974.

[11] R. W. Farquhar, "Mission Strategy for Cometary Exploration in the 1980's", Proceedings of IAU Colloquium No. 25, November 1974.

[12] R. W. Farquhar, F.I. Mann, D.P. Muhonen, and D.K. Yeomans, "Multi-Comet Intercept Missions Via Earth Swingby," To be published.